Quaternary International xxx (2017) 1–21

Contents lists available at ScienceDirect

Quaternary International

journal homepage: www.elsevier.com/locate/quaint

Geoarchaeological investigations of a prominent quay wall in ancient Corcyra – Implications for harbour development, palaeoenvironmental changes and tectonic geomorphology of Corfu Island (Ionian Islands, Greece)

Claudia Finkler [a, *], Kalliopi Baika [b, c], Diamanto Rigakou [d], Garyfalia Metallinou [d], Peter Fischer [a], Hanna Hadler [a], Kurt Emde [a], Andreas Vött [a]

[a] Institute of Geography, Johannes Gutenberg-Universität Mainz, Johann-Joachim-Becher-Weg 21, 55099, Mainz, Germany
[b] Centre Camille Jullian, Aix-Marseille Université CNRS (UMR 7299), MMSH, 5 Rue Château de l'Horloge, 13090, Aix-en-Provence, France
[c] Ephorate of Underwater Antiquities, Hellenic Ministry of Culture, Greece
[d] Ephorate of Antiquities of Corfu, 11 Armeni Vraila, 49100, Kerkyra, Greece

ARTICLE INFO

Article history:
Received 10 March 2016
Received in revised form
26 April 2017
Accepted 5 May 2017
Available online xxx

Keywords:
Harbour geoarchaeology
Palaeotsunami
Corfu
Tectonic geomorphology
Co-seismic uplift
Quay wall

ABSTRACT

In antiquity, the harbour-city of Corcyra (modern: Corfu) was a prevailing naval power in the Mediterranean and had several harbours to host a considerable fleet. Today, these harbours are totally or partly silted and concealed under modern urban infrastructure. Comprehensive geoarchaeological studies were conducted on the northeastern fringe of the Analipsis Peninsula where excavations have revealed the archaeological remains of a massive quay wall (Pierri and Arion sites). These remains are located east of known ancient harbour structures that belong to the Alkinoos Harbour. Our study aimed to reconstruct the palaeoenvironmental setting of the harbour facilities at the Pierri site, including the analysis of the local sedimentary record in order to detect and differentiate natural and man-made triggers that caused environmental shifts. At the Pierri site, we found geoarchaeological evidence for an ancient harbour basin related to the prominent quay wall. Associated harbour sediments indicate a protected harbour which was developed from an open shallow marine environment, most probably by the construction of breakwaters. Harbour deposits were dated using radiocarbon analyses and diagnostic ceramic fragments to the 4th to 3rd cent. BC. This is in good agreement with the age of the harbour installations as such archaeologically assigned to the Classical and Hellenistic period. The Pierri site was possibly in function as a harbour facility even before the 4th cent. BC. In any case, it was strongly hit by an earthquake and associated tsunami event during Classical to Hellenistic times. By this event, the harbour was uplifted and covered by event deposits so that it was not usable any more. It was subsequently buried by anthropogenic and colluvial sediments. Overall, the Pierri coastal archive allowed to identify three distinct tsunami landfall events, namely before 2483–2400 cal BC (event I), after 2483–2400 cal BC and before 370–214 cal BC (event II), and during Classical to Hellenistic times, most probably between the 4th and 3rd cent. BC (event III). Another tsunami event (event IV) potentially hit the site when it was dry land. Ages of tsunami events I–II and candidate tsunami IV are consistent with tsunamis known from the coasts of western Greece and southern Italy and where thus classified as supra-regional tele-events. Event III was identified as associated to a local earthquake and tsunami by which Corfu Island was uplifted and, at the same time, tilted with a vertical offset of 1.74 m from W to E.

1. Introduction

In the Mediterranean, early seafaring took probably place as early as in the Middle Palaeolithic (Ferentinos et al., 2012). However, in antiquity harbours played a major role for colonization,

* Corresponding author.
E-mail address: c.finkler@geo.uni-mainz.de (C. Finkler).

http://dx.doi.org/10.1016/j.quaint.2017.05.013
1040-6182/

trade and military expansion and were the hubs of local, regional and supra-regional traffic systems. Originally installed as basic utilitarian facilities enabling the transportation of goods, harbours evolved as fundamental structures of coastal cities and ensured extensive trade activities and economic welfare. Even those ancient cities that were located further inland spared no effort to obtain access to the sea and harbour infrastructure. Thus, harbours existed in large numbers and were the direct expression of power.

Early travellers and savants of early modern times were the first to describe ancient harbours after they had been buried in oblivion for hundreds of years. During the past two centuries, however, historians and archaeologists became more and more intrigued by ancient harbours, giving rise to profound scientific harbour research (Lehmann-Hartleben, 1923; Blackman, 1982). Modern harbour geoarchaeology has evolved during the past three decades. It is a young, rapidly emerging and growing discipline that experiences increasing attention (e.g. Marriner and Morhange, 2007).

Harbour basins represent rich geoarchaeological archives that can be used to detect manifold past environmental changes. In ancient harbours, particularly suitable indicators for palaeoenvironmental reconstructions such as pollen, microfauna, charcoal or plant remains are preserved (Marriner and Morhange, 2006; Morhange et al., 2014). Apart from sedimentological aspects, harbour-related facilities such as quays, breakwaters, fortification walls or towers, slipways and shipsheds (e.g. Blackman, 2013; Baika, 2003, 2013a) might also bear relevant information concerning palaeoenvironmental conditions and the overall set-up of the harbour complex (Baika, 2013b, 2015; Stiros and Blackman, 2014).

Today, ancient harbours are either submerged and partly eroded or landlocked, now often lying distant from the present coastline. Both is due to extensive coastal changes that took place since the time they were in use (Blackman, 1982; Vött and Brückner, 2006; Vött, 2007; Brückner et al., 2010). Among the natural factors, why harbour basins lost their functionality and were finally abandoned, gradual relative sea level changes and strong siltation but also extreme events like co-seismic uplift or destruction by earthquakes and tsunamis are the most prominent.

Regarding these extreme events, the island of Corfu is located in a key position between the seismically relatively stable Adriatic Sea (D'Agostini et al., 2008; Di Bucci and Angeloni, 2013) and the Ionian Sea, one of the most seismically active regions in the Mediterranean (Sachpazi et al., 2000, Fig. 1). Uplifted and submerged notches document that coastal changes on Corfu can be linked to earthquakes (Pirazzoli et al., 1994; Evelpidou et al., 2014; Mastronuzzi et al., 2014). On Corfu, there is also geoscientific evidence of repeated tsunami landfall as shown by recent investigations in near-coast lagoonal environments (Fischer et al., 2016a) and documented by traces of historical tsunami events recorded in the Roman Alkinoos harbour (Finkler et al., 2017). Ever since, ancient harbours are well-known as excellent sediment traps for extreme wave events such as tsunami inundation (e.g. Vött et al., 2011a; Bony et al., 2012; Hadler et al., 2013, 2015).

However, ancient harbours of Corfu were subject to only few geoarchaeological studies so far (Finkler et al., 2017). This is surprising as ancient Corcyra, located on the east coast of Corfu Island, was part of an extensive trade network in the Adriatic and Ionian Seas since the Archaic period. Moreover, it was one of the first city states throughout the Mediterranean to construct a large fleet of warships requiring harbour facilities to store and repair them. According to ancient sources, Corcyra had at least two harbours with associated infrastructure, namely the Alkinoos Harbour in the north and the Hyllaikos Harbour in the southwest of the Analipsis Peninsula (Fig. 2A; Lehmann-Hartleben, 1923; Kiechle, 1979; Baika, 2013a). A third harbour, mentioned by Skylax (Per. 29) and probably referred to by Thucydides (3.75.5, after Dent, 1910), may be located at the northeastern fringe of the city (Riginos et al., 2000; Baika, 2003). The Alkinoos Harbour in the north is well documented in an archaeological context and provides an excellent archive for geoarchaeological research (Finkler et al., 2017). Yet, the overall harbour topography along the entire northern part of the peninsula is complex and difficult to understand. In any case, a number of specific archaeological remains of harbour-related infrastructure (Baika, 2013a) are reliable indicators to reconstruct the ancient harbour setting along the northern fringe of the Analipsis Peninsula.

The present study focusses on the Pierri site at the northern fringe of the Analipsis Peninsula where distinct elements of ancient harbour facilities were found within the framework of archaeological excavations, such as a section of a quay wall, probably associated with a presumed ramp structure. Together with the associated sedimentary record, the harbour site represents a promising setting where complex interactions between man-made infrastructure and palaeoenvironmental changes have been recorded. We conducted detailed investigations of the sedimentary record in this part of the harbour in order (i) to reconstruct the palaeoenvironmental setting for the time when the harbour facilities were used, (ii) to identify coastal changes and relative sea level fluctuations in the late Holocene and their major triggering factors, and (iii) to check whether the harbour can be used to reconstruct seismo-tectonic events, such as tsunami impacts, co-seismic crust movements and tectonic influences.

2. Regional setting

2.1. Natural setting

Corfu is located in the northern Ionian Sea, close to the Street of Otranto which is the entrance to the Adriatic Sea. Corfu is the northernmost island of the Ionian archipelago where all types of plate boundaries can be observed within a distance of only 100 km (Fig. 1A; Sachpazi et al., 2000). In the north, the eastern coasts of the Adriatic Sea are under the influence of both subsidence and uplift due to the continent-continent collision caused by the movement of the Adriatic Microplate towards the Eurasian Plate (Babbucci et al., 2004; Suric et al., 2014). The Ionian Sea itself is situated between the subduction zones of the Calabrian Arc in the southwest and the Hellenic Arc in the southeast (van Hinsbergen et al., 2006; Hollenstein et al., 2008). Both systems, the subduction zones in the south and the collision belt in the north, are separated by the Cefalonia Transform Fault (CTF), a large dextral strike-slip fault zone right south of Corfu (Kokkalas et al., 2006), and the Kerkyra-Cefalonia submarine valley system with associated faults as northern branch of the Ionian subduction zone (Poulos et al., 1999).

Corfu Island is therefore located within an exceptional tectonic stress field resulting in the Corfu thrust, a NNW-SSE running compressional structure on the island, accompanied by frequent shallow focus earthquakes (van Hinsbergen et al., 2006; Kokkalas et al., 2006). They reach moment magnitude values around 6 (Stucchi et al., 2013) and are documented by several entries in earthquake and tsunami catalogues since medieval times (Partsch, 1887; Soloviev et al., 2000; Ambraseys and Synolakis, 2010; Hadler et al., 2012).

Pirazzoli et al. (1994) and Evelpidou et al. (2014) detected emerged coastal notches on Corfu and satellite islands indicating co-seismic uplift. The notches on Corfu document at least two periods of crust uplift for the central and western part of the island. The first is dated to the 8^{th}–4^{th} cent. BC, while the second event has remained undated so far. Mastronuzzi et al. (2014) suggests a tectonic up- and down movement of the island. They also describe

Please cite this article in press as: Finkler, C., et al., Geoarchaeological investigations of a prominent quay wall in ancient Corcyra – Implications for harbour development, palaeoenvironmental changes and tectonic geomorphology of Corfu Island (Ionian Islands, Greece), Quaternary International (2017), http://dx.doi.org/10.1016/j.quaint.2017.05.013

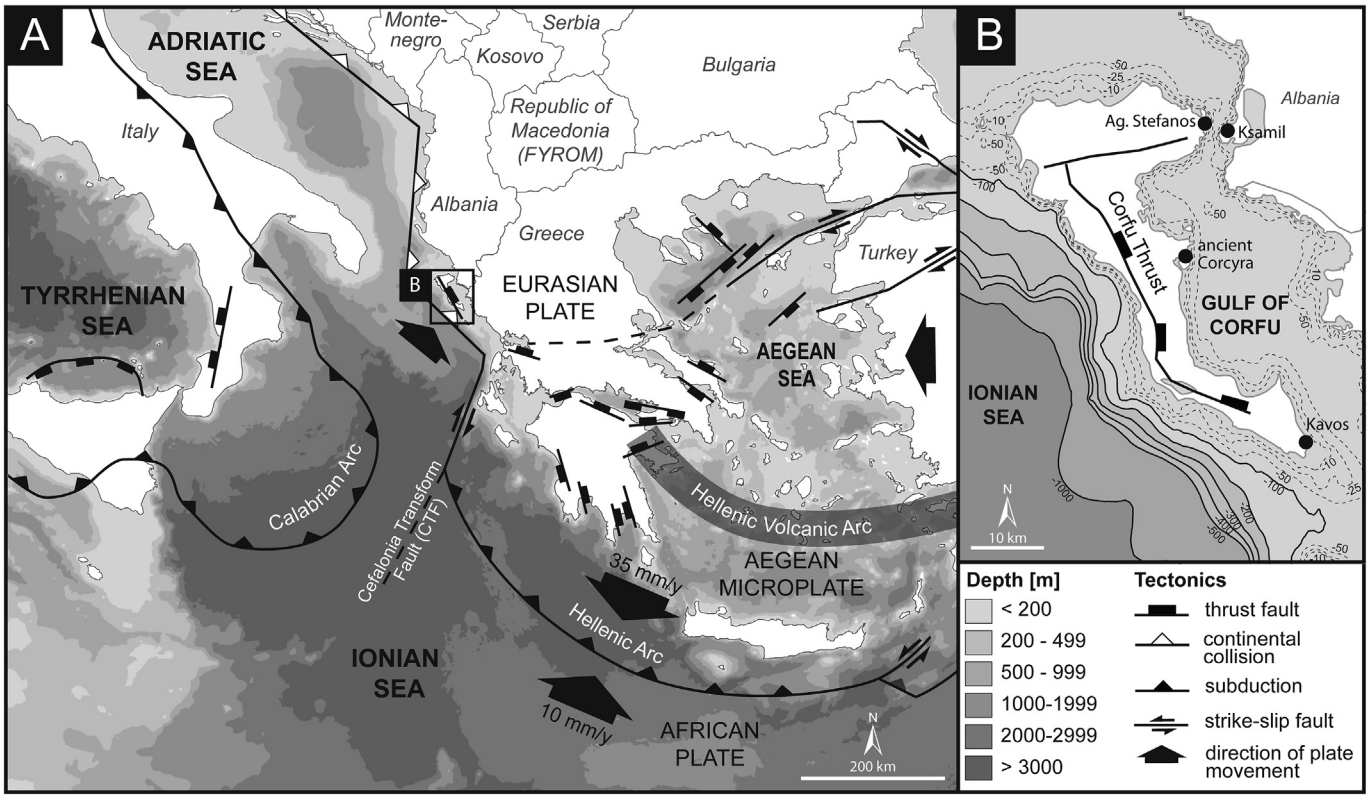

Fig. 1. Tectonic structures and bathymetric conditions in the eastern Mediterranean. (A) Simplified tectonic map of the Ionian, Adriatic and Aegean Seas. Corfu Island (black box) is exposed to the Adriatic continental collision belt in the north, the subduction zones of the Hellenic and Calabrian Arc in the South and the Cefalonia Transform fault (CTF) right southwest of the island. Owing to compressional tectonics, the Corfu thrust as normal fault runs across the island. (B) Simplified bathymetry map of Corfu Island. While the lake-like Gulf of Corfu (Partsch, 1887) between the island and the Greek/Albanian mainland features water depths of less than 70 m, the steep continental slop west of Corfu reaches more than 1000 m water depth. Main tectonic structures after Billi et al. (2007), Doutsos and Kokkalas (2001); bathymetry after GEBCO (2014).

further earthquakes and assume associated tsunami inundations, for example at around 1000 cal BC, contemporaneous with a tsunami landfall reported from northwestern Greece (Vött et al., 2006, 2011b).

On Corfu, Fischer et al. (2016a) detected geomorphological and microfaunal traces of multiple tsunami inundation in near-coast lagoons, proving Corfu's sensitivity towards tsunami events, and Finkler et al. (2017) present geoscientific evidence of historical

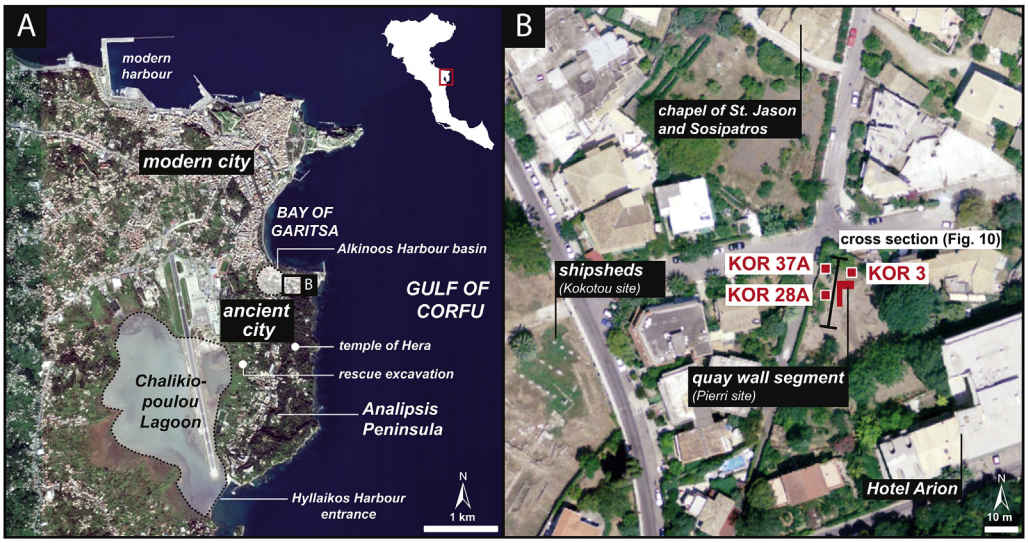

Fig. 2. Topographic overview and detailed map of the study area. (A) Corfu city is situated at the eastern shore of the island and separated from the Greek and Albanian mainland by the Gulf of Corfu. Ancient Corcyra was built on the Analipsis Peninsula between the Chalikiopoulou Lagoon in the southwest and the Bay of Garitsa in the north. (B) The area associated with the ancient Alkinoos Harbour, traced by archaeological remains of shipsheds (Kokotou site), lies c. 200 m distant to the present coastline. At the Pierri site, remains of a quay wall document the use as a harbour (Baika, 2013a,b). Vibracoring sites are marked by red rectangles. Map modified after Bing aerial image of the year 2016 and NCMA S.A. (2014). (For interpretation of the references to colour in this figure legend, the reader is referred to the web version of this article.)

Please cite this article in press as: Finkler, C., et al., Geoarchaeological investigations of a prominent quay wall in ancient Corcyra – Implications for harbour development, palaeoenvironmental changes and tectonic geomorphology of Corfu Island (Ionian Islands, Greece), Quaternary International (2017), http://dx.doi.org/10.1016/j.quaint.2017.05.013

tsunami impact to the Roman Alkinoos Harbour. Palaeotsunami signatures in coastal geoarchives are also reported from the other Ionian Islands (Hadler et al., 2011; May et al., 2012; Willershäuser et al., 2013), the northern Greek mainland (Vött et al., 2009, 2010, 2011b), and the Italian coasts of the Ionian and Adriatic Seas (Gianfreda et al., 2001; Mastronuzzi et al., 2007; Smedile et al., 2011; De Martini et al., 2012). Local seismic events might also cause submarine debris flows, mainly bound to the slopes of the Kerkyra-Cefalonia valley system and the steep continental slope to the west of Corfu (Fig. 1B; Poulos et al., 1999).

The wind and wave climate of the northern Ionian Sea is dominated by mainly westerly winds and low significant wave heights with average values of less than 1 m (Cavaleri, 2005; Lionello et al., 2012). During winter season, storms occur frequently, often linked to Sirocco or tropical-type cyclones, so-called medicanes (Llasat, 2009). Even though the track lines of such medicanes usually run further south, they are a known phenomenon in the northern Ionian Sea (cf. Davolio et al., 2009). Due to the prevailing westerly winds, it is mainly the western coast of Corfu, facing the open Ionian Sea, which is affected by such conditions. In contrast, the eastern shores of the island with the ancient city of Corfu (Corcyra) and its harbours adjoin the Gulf of Corfu. The Gulf of Corfu has water depths of less than 70 m and is described as almost lake-like (Partsch, 1887; Fig. 1B) with a very weak wave climate (Mazarakis et al., 2012; Zacharioudaki et al., 2015). Topographically, ancient Corcyra is located on the Analipsis Peninsula (Fig. 2A) which separates the Chalikiopoulou Lagoon in the west from the Bay of Garitsa in the east. The peninsula is built of Miocene marls (IGME, 1970) forming a ridge up to 60 m high.

2.2. Archaeological and historical background

Ancient Corcyra was founded as a Corinthian colony in the late 8th cent. BC due to its strategic position between the Adriatic and Ionian Seas along the sea routes between Greece and Italy (Kiechle, 1979). Soon, the former colony emerged as a prevailing naval power in the Mediterranean, documented by its participation in the first naval battle ever recorded in Greek history in 664 BC against its metropolis Corinth (Thucydides 1.13.4 after Dent, 1910). Corcyra was one of the first Mediterranean city states that invested in a considerable fleet of triremes and appropriate harbour infrastructure (Baika, 2013a). According to Thucydides (1.25.4, after Dent, 1910), Corfu is supposed to have owned at least 120 ships before the Peloponnesian War.

The Archaic polis of Corcyra evolved on the naturally fortified Analipsis Peninsula, where the remains of several sanctuaries, such as the Heraion, one of the earliest major temples in Greece (Sapirstein, 2012), are still preserved (Figs. 2A and 11). From here, the city extended towards the western and northern hill slopes into the coastal lowlands where the harbours of the city were situated according to ancient sources (Schmidt, 1890; Lehmann-Hartleben, 1923; Baika, 2003). While two of the ports, the military Alkinoos Harbour in the Bay of Garitsa and the Hyllaikos Harbour on the eastern shore of the Chalikiopoulou Lagoon (Fig. 2A), are well documented in an archaeological context (Partsch, 1887; Dontas, 1965; Kanta-Kitsou, 2001; Baika, 2013a), a third harbour suggested along the northern fringe of the peninsula remains conjectural (Riginos et al., 2000; Gehrke and Wirbelauer, 2004; Baika, 2013a).

The present study focuses on remains of harbour facilities at the so called Pierri site on the northeastern coast of the peninsula. West of it, at the Kokotou site, the basin of the Alkinoos Harbour, though silted, can be traced by harbour infrastructure which developed on its shore, namely a section of a monumental complex of trireme shipsheds (Fig. 2B) dating to the early 5th cent. BC (Preka-Alexandri, 1986; Spetsieri-Choremi, 1997; Baika, 2003, 2013a). This shipshed complex was excavated in the 1980s and 1990s and has been subject to geoarchaeological research (Finkler et al., 2017), still ongoing. At the Pierri site, located approximately 80 m to the east of the shipsheds, recent rescue excavations brought to light remains of a continuous W-E running quay wall (Fig. 3). This quay is interrupted by slipways or ramps that slope towards the sea at regular intervals (Riginos et al., 2000; Fig. 3). The prolongation of the quay wall and ramp system towards the east of the Pierri site is nowadays covered by modern buildings, for example by the Hotel Arion complex. Here, the most significant section of the quay wall was excavated before the construction of the hotel (Arion site, Fig. 2B).

Structurally, the quay wall section at the Pierri site is made out of white limestone ashlars and characterised by a corner with a vertically disposed branch, orientated north-south. This wall section seems to be the lateral delimitation of a ramp, today covered by younger deposits. The western part of the presumed ramp is assumed under a modern road construction (Fig. 2B). The archaeological remains found at the Pierri site are yet unpublished. Geoarchaeological and geomorphological investigations presented in this paper considerably enhance the understanding of the evolution of the harbour environment.

The northern harbour zone was heavily used and modified since the destruction of the city by the Roman troops of Agrippa in 31 BC, right before the battle near Actium. In Roman times, the harbour basins were partly covered with debris from different remodelling phases of the city. Moreover, some sections of the harbour area were used as a cemetery, reshaping the pre-Roman structures and deposits. Remains of Roman residential quarters and warehouses have been sporadically unearthed lying on top of Classical and Hellenistic structures (Riginos et al., 2000; Baika, 2013a).

In general, the seaward shift of the coastline since antiquity and modern urban building activities have concealed the harbour topography. At the Pierri site, the quay structure is located more than 200 m distant from the present coastline (Fig. 2), bearing witness of significant palaeogeographical changes. Due to the extensive urban development of the modern city, the archaeological reconstruction of the northern harbour topography is still conjectural. It is still unclear if all known remains of harbour facilities, such as the Kokotou shipsheds and the Pierri and Arion quay wall sections, belonged to one and the same harbour, namely the Alkinoos Harbour. Even in case they did, we are uncertain on the overall form, extent and topographical configuration of this harbour. However, all these harbour facilities may be of the same age or may have been used simultaneously for a certain period of time, in particular during the Classical and Hellenistic periods (5th to 1st cent. BC). Archaeological research needs to be intensified to clarify their precise ages.

3. Methods

This study used a multi-methodological approach including sedimentological, geochemical and microfaunal methods in order to reconstruct palaeoenvironmental conditions of the harbour environment at the Pierri site.

Vibracoring was conducted to retrieve the stratigraphical sequence in the context of archaeological structures. Three vibracores covered all relevant parts of the Pierri site, namely the landward area of the assumed ramp, its seaward continuation and the area right in front of the excavated quay wall section (Figs. 2B and 3). We used an automotive drill rig (Nordmeyer RS 0/2.3) and a handheld vibracorer (Atlas Copco Cobra mk 1) with core diameters of 50–80 mm. Vibracores were cleaned, photographed, described and sampled with regard to stratigraphical units. Selected vibracores (suffix “A”) were drilled using plastic liners to

Please cite this article in press as: Finkler, C., et al., Geoarchaeological investigations of a prominent quay wall in ancient Corcyra – Implications for harbour development, palaeoenvironmental changes and tectonic geomorphology of Corfu Island (Ionian Islands, Greece), Quaternary International (2017), http://dx.doi.org/10.1016/j.quaint.2017.05.013

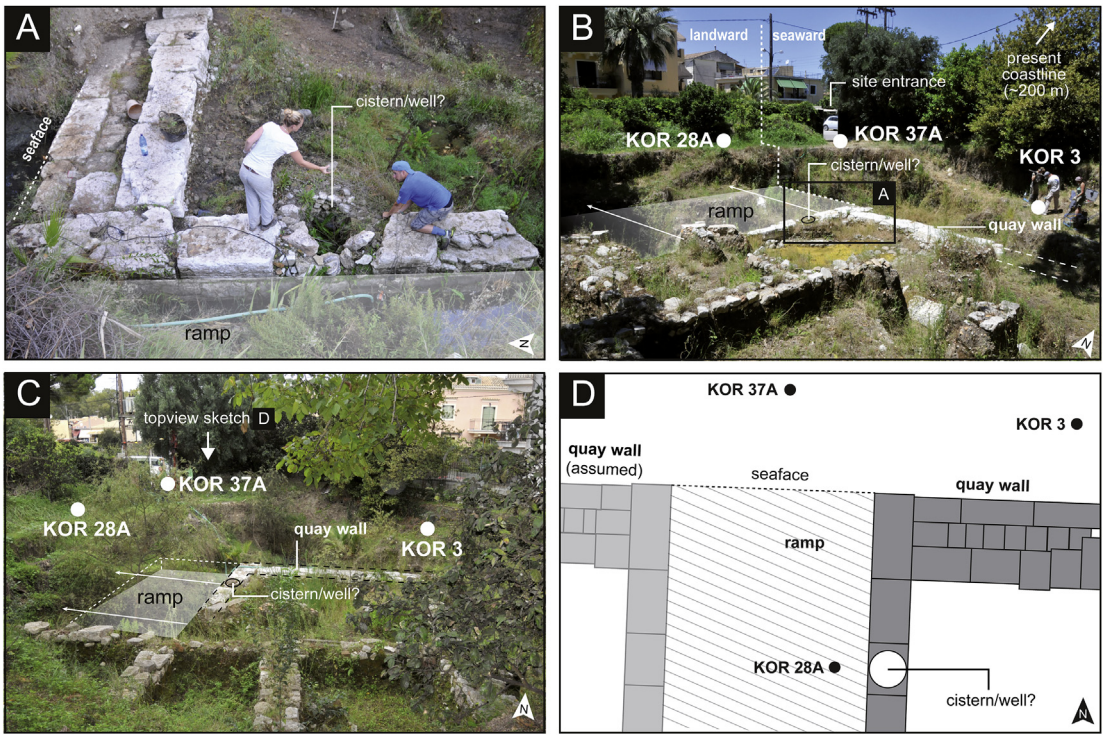

Fig. 3. Photographic overview of the Pierri site. (A) Detailed view of the quay wall segment and vertical wall section, excavated at the Pierri site. View to the east. (B), (C) Location of vibracoring sites in relation to the Pierri quay wall and the associated ramp. View to the northwest and north, respectively. Vibracore KOR 28A was drilled on the landward site of the quay, covering the area of the assumed ramp, while vibracore KOR 3 is situated seaward right in front of the quay wall. Vibracoring site KOR 37A was drilled right in front of the assumed ramp. (D) Simplified sketch (top view, not true to scale) of the Pierri Site quay wall segment with associated ramp. (Photos by A. Vött).

enable high-resolution in-situ measurements in the laboratory. At vibracoring site KOR 37A, in-situ Direct Push Electrical Conductivity (DP EC) logging was conducted. The used DP EC probe (Geoprobe SC520) had four electrodes in a linear Wenner arrangement to measure electrical conductivity and the rate of penetration every 2 cm (Schulmeister et al., 2003; Harrington and Hendry, 2006; Fischer et al., 2016b).

Position and elevation of vibracoring and DP EC sites were determined by means of a differential GPS (Topcon HiPer Pro FC-250).

In the laboratory, grain size distribution of samples from selected sediment layers was analysed using the Köhn method (Köhn, 1929; DIN ISO 11277, 2002; Blume et al., 2011). After separating skeletal components >2 mm, each subsample of 15 g was first pretreated by H_2O_2 and dispersants. The amounts of clay and silt were determined by pipetting, while sand was analysed by dry-sieving. Magnetic susceptibility was measured using a Bartington Instruments MS3 with a MS2K surface sensor. Laboratory work also comprised X-ray fluorescence (XRF) analyses by means of a portable Niton XL3t 900S GOLDD (calibration mode SOIL) instrument, yielding concentrations of Ca, Fe, Pb and more than 25 other elements. Measurements were conducted in-situ on the undisturbed sediment cores with an average resolution of 2 cm. Data obtained by handheld XRF devices, analogues to data obtained by XRF core scanners, are considered to be of semi-quantitative nature because of matrix effects. Such matrix effects may be due to possible variations in particle size, uniformity, surface geometry and moisture (EPA, 2007; Chagué-Goff et al., 2017). Compared to alternative analysing methods, absolute elemental concentrations might be slightly differing and/or shifted to higher or lower levels depending on such matrix effects (Argyraki et al., 1997; Shefsky, 1997). To ensure comparison, we therefore preferred elemental ratios and focussed on distinct shifts in general distribution patterns and overall trends of elemental concentrations that indicate major changes in palaeoenvironmental conditions. Geochemical analyses based on pXRF are an approved and accepted tool in palaeoenvironmental research (Judd et al., 2017).

Selected sediment samples from vibracores KOR 28A and KOR 37A were examined regarding their microfaunal content. We mainly concentrated on foraminifera as they occur under marine to rarely brackish conditions and thus represent excellent indicators for the reconstruction of different palaeoenvironmental settings due to their different ecological requirements (Murray, 1991, 2006). Thus, foraminiferal assemblages help to differentiate between abrupt and gradual changes as well as to detect allochthonous interferences (Dominey-Howes et al., 2000; Mamo et al., 2009; Pilarczyk et al., 2014). In the frame of the presented study, 15 ml of sediment from each sample were pretreated with H_2O_2 and sieved into fractions of >400 μm, >200 μm and >125 μm. We used up to 5 ml of sample material for a semi-quantitative microfaunal analysis. Foraminifera were counted and determined after Loeblich and Tappan (1988) and Cimermann and Langer (1991) using a stereo microscope. Species were classified according to their habitat preferences after Murray (1991, 2006) and Sen Gupta (1999). Additionally, photos of selected specimens were taken using a scanning electron microscope (SEM).

Altogether ten organic samples were dated by means of ^{14}C-AMS analysis, which was accomplished at the Klaus-Tschira Laboratory of the Curt-Engelhorn-Centre Archaeometry gGmbH Mannheim, Germany (MAMS), and the Keck Carbon Cycle AMS Facility, University of California at Irvine, USA (UCI; Table 3). Five samples of charcoal, wood and seaweed were extracted from vibracores KOR 28A and KOR 37A in order to establish a local geochronostratigraphy of the harbour development at Pierri. This geochronostratigraphy was complemented by a local age-depth-model based on relative sea level indicators (peat, oysters) or on

Please cite this article in press as: Finkler, C., et al., Geoarchaeological investigations of a prominent quay wall in ancient Corcyra – Implications for harbour development, palaeoenvironmental changes and tectonic geomorphology of Corfu Island (Ionian Islands, Greece), Quaternary International (2017), http://dx.doi.org/10.1016/j.quaint.2017.05.013

samples that were collected right above peat-like layers; thus, the latter samples were also in close relation to the local sea level at the time of their deposition. Concretely, this model is based on two samples from vibracores that were drilled in the surroundings of the ancient city (Finkler et al., 2017) consisting of charcoal and peat, respectively. Additionally, three oyster samples were collected from a band of oysters that was found adhered to a section of the Pierri quay wall which was recently unearthed. Calibration of all samples was realised based on the software Calib 7.1 (Stuiver and Reimer, 1993; Reimer et al., 2013). Archaeological age estimates of diagnostic ceramic fragments (Table 4) were used to cross-check radiometric ages.

4. Results: stratigraphical record at the Pierri site

Three vibracores were drilled at the Pierri site (Figs. 2B and 3), including the landward area of the presumed ramp structure (vibracore KOR 28A; Figs. 4–6), its seaward continuation (vibracore KOR 37A; Figs. 7–9) and the harbour basin to the north of the quay (vibracore KOR 3; Fig. 5). Moreover, we obtained high-resolution stratigraphical data at vibracoring site KOR 37A by DP EC logging.

Vibracoring sites KOR 3, KOR 28A and KOR 37A are located in a short distance to one another, their position being closely related to the archaeological quay structure (Table 1). Vibracore KOR 3 was drilled to the immediate north of the Pierri quay wall. It shows a layer of compact silty clay at its base, covered by a thick sequence of grey fine to finest sand. At 2.77 m b.s., sediment texture changes towards silt and silty sand of dark grey colour. Towards the top, at 2.35–1.61 m b.s., a layer of gravel embedded in a sandy matrix was found followed by brownish clayey silt including cultural debris.

At the base of vibracore KOR 28A, drilled on a presumed ramp structure several meters 'inland' of the quay wall, a thick basal section of greyish fine to finest sand is intersected two times by layers of coarse sand and sandy gravel, respectively. At 4.40 m b.s., a layer of homogeneous light-grey fine sand appears which is covered by solid stones. Finally, we found a section of greyish-brownish coarse sand followed by a thick unit of clayey silt with embedded ceramics and debris that marks the upper part of the core.

The stratigraphy of vibracore KOR 37A, drilled in front of the presumed ramp and the quay wall abreast to site KOR 3, is characterised by fine to finest sand at the base. This sand layer is intersected by two layers of coarse-grained deposits, namely coarse sand and gravel. After a sharp contact at 4.63–4.17 m b.s., a sequence of very heterogeneous silty sand and silt was found, containing large amounts of organic remains and debris. Following a section of multi-coloured sandy gravels at 3.87–3.53 m b.s. a sequence of brownish clayey silt, more than 3 m thick, characterises the upper part of the core. This layer was found intersected by a comparatively thin layer of light and slightly coarser deposits.

Based on distinct similarities in grain size, colour, geochemical parameters and microfaunal content, the local sedimentary records of vibracores KOR 3, KOR 28A and KOR 37A was classified into the following stratigraphical units A to G. Due to the high variability of unit C sediments, we differentiate between eight subunits C1 to C8.

Unit A (8.85–7.00 m b.s. in KOR 3, Fig. 5) is restricted to vibracore KOR 3. It is characterised by compact silty clay of grey colour, rich in $CaCO_3$, showing medium LOI values of c. 5%.

In contrast, ***Unit B*** was found in all vibracores (6.85–2.77 m b.s. in KOR 3; 6.93–6.23, 6.06–5.75, 5.08–4.40 m b.s. in KOR 28A; 8.53–6.75, 6.36–5.65, 5.42–4.63 m b.s. in KOR 37A). It consists of greyish fine sand with minor amounts of medium and coarse sand and components >2 mm. Geochemically, the unit is characterised by a low to medium Ca/Fe ratio and a medium Sr/Rb ratio. The deposits are void of Pb and show a very low magnetic susceptibility. High-resolution DP EC logging at vibracoring site KOR 37A (Fig. 8) revealed strongly increased EC values to the base of the unit. The sand within unit B contain medium to high abundances of well-preserved marine foraminifera from different ecological habitats. However, the distribution of species shows a depth-related shift in vibracore KOR 28A: In the lower part, Miliolidae (especially *Quinqueloculina seminula*), habitants of seaweed meadows and species, tolerating also brackish water (*Ammonia tepida, A. beccarii, Haynesina depressula*) occur in high numbers. In contrast, their abundances decrease in the upper part of unit B. Instead, planktonic foraminifera and species preferring deeper and colder waters appear with increasing numbers.

Unit C is characterised by badly sorted sand with distinctly increased amounts of medium to coarse sand and skeletal components >2 mm. As sediments from this unit appear highly variable, we differentiate between the following subunits (Table 2).

Subunit C1 (6.23–6.06 m b.s. in KOR 28A, Fig. 4B) is characterised by greyish medium and coarse sand including high numbers of multi-coloured gravels and abundant marine macrofauna. To the top of the unit, grain size distribution reveals a general fining-upward tendency with a clayey mud layer, rich in organic material, on the very top. Similar to unit B, Pb and magnetic susceptibility show low values, whereas Ca/Fe and Sr/Rb ratios reveal distinct peaks, the latter even reaching the highest values within the whole profile. Palaeontologically, the coarse sand of subunit C1 is dominated by marine and seaweed assemblages with decreased numbers of Miliolidae but a slightly increased abundance of cold-marine and planktonic species like *Orbulina universa,* and *Lobatula lobatula* (Murray, 2006). Moreover, *Globigerina bulloides* and *Globigerinoides* sp. appear initially.

Subunit C2 (5.75–5.08 m b.s. in KOR 28A) was found on top of an erosive contact and is characterised by gravel embedded in a matrix of medium to coarse sand. The unit further reveals a fining upward sequence in grain size and contains plenty ceramic fragments and clasts, consisting of clayey silt. Ca/Fe and Sr/Rb values were found on a medium level with distinct peaks. In contrast to the geochemical characteristics of unit B, peaks in Pb concentration and magnetic susceptibility are visible. Microfaunal analyses indicate a similar foraminiferal fingerprint as found for unit B and subunit C1 with increased abundance of *Lenticulina* sp. and *Gyroidina soldanii*, both preferring cold-marine conditions (Murray, 2006) and missing in the sediments below.

Subunit C3 (3.87–3.52 m b.s. in KOR 28A) features greyish to brownish coarse sand with considerable amounts of medium sand and gravel. The sand contains various marine macrofauna, ceramics and charcoal. While Ca/Fe and Sr/Rb ratios are very similar to those of the underlying units, Pb contents reach medium to high values. Moreover, magnetic susceptibility increases distinctly. The microfaunal fingerprint strongly resembles unit D: seaweed-related and especially (shallow) marine species occur only in small numbers. Instead, cold-marine and brackish species are dominant.

Subunit C4 (6.75–6.36 m b.s. in KOR 37A) overlies unit B on top of an erosional contact and is formed of grey fine to coarse sand, containing considerable amounts of components >2 mm, such as gravels and ceramics. The amount of skeletal material decreases upward, concurrently grain size (<2 mm) fines upward as well. The sediments show the same geochemical and microfaunal signals as unit B except for magnetic susceptibility and Pb, where distinct peaks are visible.

Subunit C5 (5.65–5.42 m b.s. in KOR 37A) is characterised by gravel within a matrix of medium and coarse sand. Ca/Fe and Sr/Rb ratios were found on a medium level, while magnetic susceptibility as well as Pb values are distinctly increased. Regarding their microfaunal content, the sediments do not significantly differ from those of unit B.

Please cite this article in press as: Finkler, C., et al., Geoarchaeological investigations of a prominent quay wall in ancient Corcyra – Implications for harbour development, palaeoenvironmental changes and tectonic geomorphology of Corfu Island (Ionian Islands, Greece), Quaternary International (2017), http://dx.doi.org/10.1016/j.quaint.2017.05.013

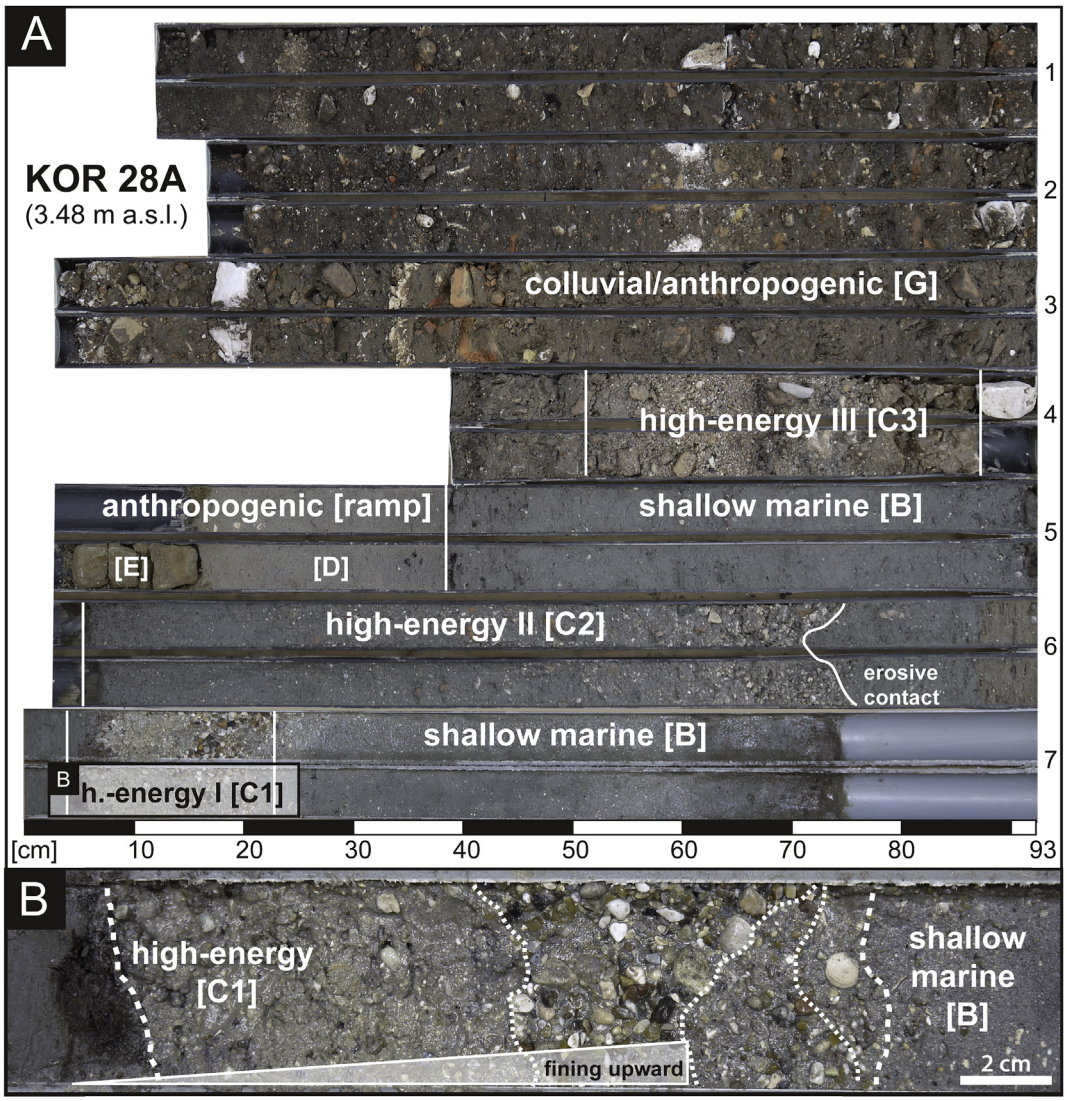

Fig. 4. Stratigraphical record of vibracore KOR 28A. (A) On top of a thick unit of shallow marine sand, intersected by two high-energy layers (I and II), a solid ashlar out of calcareous sandstone and underlying homogeneous fine sand mark the base of the ramp at the Pierri site. It is covered by sediments of a high-energy facies (event III) and subsequent sediments of colluvial to anthropogenic origin. Capital letters B–G represent associated stratigraphical units; see text for explanation. (B) Detailed photo of high-energy deposits (event I, 6.61–6.06 m b.s) intersecting shallow marine sands. Mark the fining upward tendency in grain size and the peat-like sediments on top.

Subunit C6 (3.87–3.53 m b.s. in KOR 37A) represents a poorly sorted sequence of gravel towards coarse sand and silt with embedded macrofossils and ceramics. While Sr/Rb values are similar to those of the underlying unit B, the Ca/Fe ratio is strongly decreased similar to the one of unit F. In addition, Pb concentration and magnetic susceptibility show distinct peaks. The foraminiferal content is dominated by low diversity and abundance of mainly *Ammonia* spp., *Gyroidina soldanii and Globigerinoides* sp.

These species are also abundant in ***subunit C7*** (1.79–1.64 m b.s. in KOR 37A), which is intersecting a thick sequence of unit G in vibracore KOR 37A. Apart from different microfaunal content and a slightly increased amount of medium and coarse sand the unit does not differ strongly from unit G.

Subunit C8 (2.35–1.61 m b.s. in KOR 3) is formed by gravel embedded in a matrix of medium to coarse sand with only low amounts of clay and silt. The unit features a basal erosional contact and contains high amounts of ceramic sherds and marine macrofauna.

Unit D was only found in vibracore KOR 28 (4.40–4.17 m b.s. in KOR 28A). It is characterised by homogeneous light-grey fine sand with minor amounts of clay, silt and coarser sands. Geochemically, this unit strongly resembles unit B, whereas its microfaunal fingerprint differs significantly. Apart from planktonic species and *Ammonia beccarii* only few other species appear in very low abundance.

Unit E (4.17–3.87 m b.s. in KOR 28A) is characterised by solid calcareous sandstone of yellowish colour, overlain by white limestone.

Unit F, located at the same elevation level as units D and E, appears in vibracores KOR 3 and KOR 37A (2.77–2.35 m b. and 4.63–4.17 m b.s., respectively). In vibracore KOR 37A, the unit overlies the underlying unit B on top of a sharp contact. The unit itself is dominated by poorly sorted silt to silty sand. It further contains considerable amounts of medium sand, ceramics, marine macrofossils and plenty of seaweed. LOI values are strongly, Pb values slightly increased. Microfaunal analyses revealed high diversity especially in the lower section. Foraminifera tolerant to brackish conditions (Murray, 2006), such as *Ammonia beccarii, A. tepida* and *Haynesina depressula,* as well as species of seaweed assemblages, such as *Rosalina* sp., *Planorbulina mediterranea* or

Please cite this article in press as: Finkler, C., et al., Geoarchaeological investigations of a prominent quay wall in ancient Corcyra – Implications for harbour development, palaeoenvironmental changes and tectonic geomorphology of Corfu Island (Ionian Islands, Greece), Quaternary International (2017), http://dx.doi.org/10.1016/j.quaint.2017.05.013

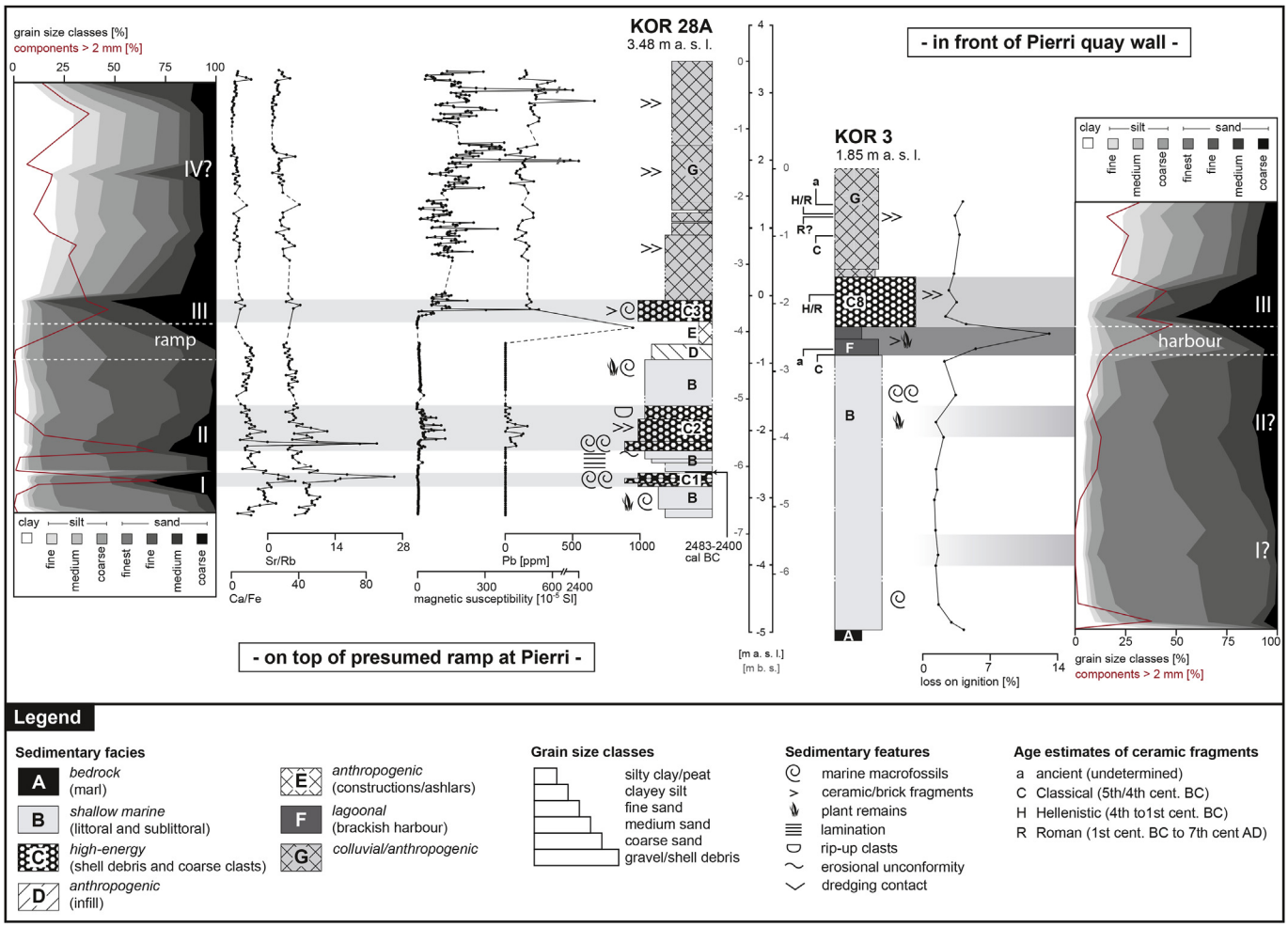

Fig. 5. Results from grain size analysis, magnetic susceptibility measurements and selected geochemical proxies of vibracores KOR 28A (left) and KOR 3 (right). Lagoon-type harbour deposits (highlighted by dark grey colour) in vibracore KOR 3 were found in a stratigraphical position consistent with anthropogenic deposits marking most likely the base of a ramp. High-energy layers (highlighted by light grey colour) are characterised by increased amounts of medium to coarse sand but show different geochemical fingerprints.

Peneroplis sp. were found.

Finally, ***unit G*** (1.61–0.00 m b.s. in KOR 3; 3.52–0.00 m b.s. in KOR 28A; 3.53–1.79, 1.64–0.00 m b.s. in KOR 37A) consists of brownish clayey silt including high amounts of cultural debris and charcoal and characterises the upper part of the cores. Pb concentrations and magnetic susceptibility are distinctly increased but strongly fluctuating. Apart from *Orbulina universa*, *Globigerina bulloides* and *Globigerinoides* sp., only few strongly-weathered species were found within this unit.

5. Interpretation and discussion

5.1. Facies interpretation

Based on their geochemical, microfaunal and grain-size related characteristics, the different units retrieved from the Pierri site sedimentary record can be associated to the following sedimentary facies:

Unit A is identified as Neogene marl that forms the ***bedrock*** at a depth of approximately 5 m b.s.l. at the Pierri site. These Neogene marls crop out in the south of the Analipsis Peninsula, forming a ridge up to 60 m high (Fig. 2A; IGME, 1970). However, the presence of Neogene marls is problematic with regard to its microfaunal signature as reworked older fossils might contaminate younger, Holocene deposits. In order to separate potentially reworked Neogene bedrock species from Holocene fauna, we analysed several bedrock samples regarding their microfaunal content (e.g. Finkler et al., 2017). Apart from planktonic species, already known from literature (cf. IGME, 1970), we found several cold-marine species such as *Lenticulina* sp. and *Uvigerina mediterranea* within the local bedrock (please see species classification in Figs. 6 and 9). These species must be regarded as potentially reworked and are thus considered as geogenic background signal.

Grain size and geochemical characteristics of unit B sediments indicate a mid-energy littoral environment. ***Shallow marine*** conditions are reflected by foraminiferal assemblages containing high numbers of calcareous marine and seaweed-related species, typical of shallow (some 10 m) inner-shelf bays with normal marine salinity and stable temperate to high water temperatures (Murray, 1991, 2006; Sen Gupta, 1999). The lower part of the shallow marine fine sands shows a changed pore water geochemistry due to salt water influence, represented by steadily increasing DP-EC values in vibracore KOR 37A.

Unit C and associated sublayers are characterised by distinct coarser grain sizes depicted by input of medium and coarse sand as well as gravel, suggesting ***high-energy*** conditions, especially when compared to the basal shallow marine sands. Based on the sedimentary signatures of unit C deposits, the material originates from shallow marine and/or marine environments partly also including reworked lagoonal material. Unit C thus indicates event-related

Please cite this article in press as: Finkler, C., et al., Geoarchaeological investigations of a prominent quay wall in ancient Corcyra – Implications for harbour development, palaeoenvironmental changes and tectonic geomorphology of Corfu Island (Ionian Islands, Greece), Quaternary International (2017), http://dx.doi.org/10.1016/j.quaint.2017.05.013

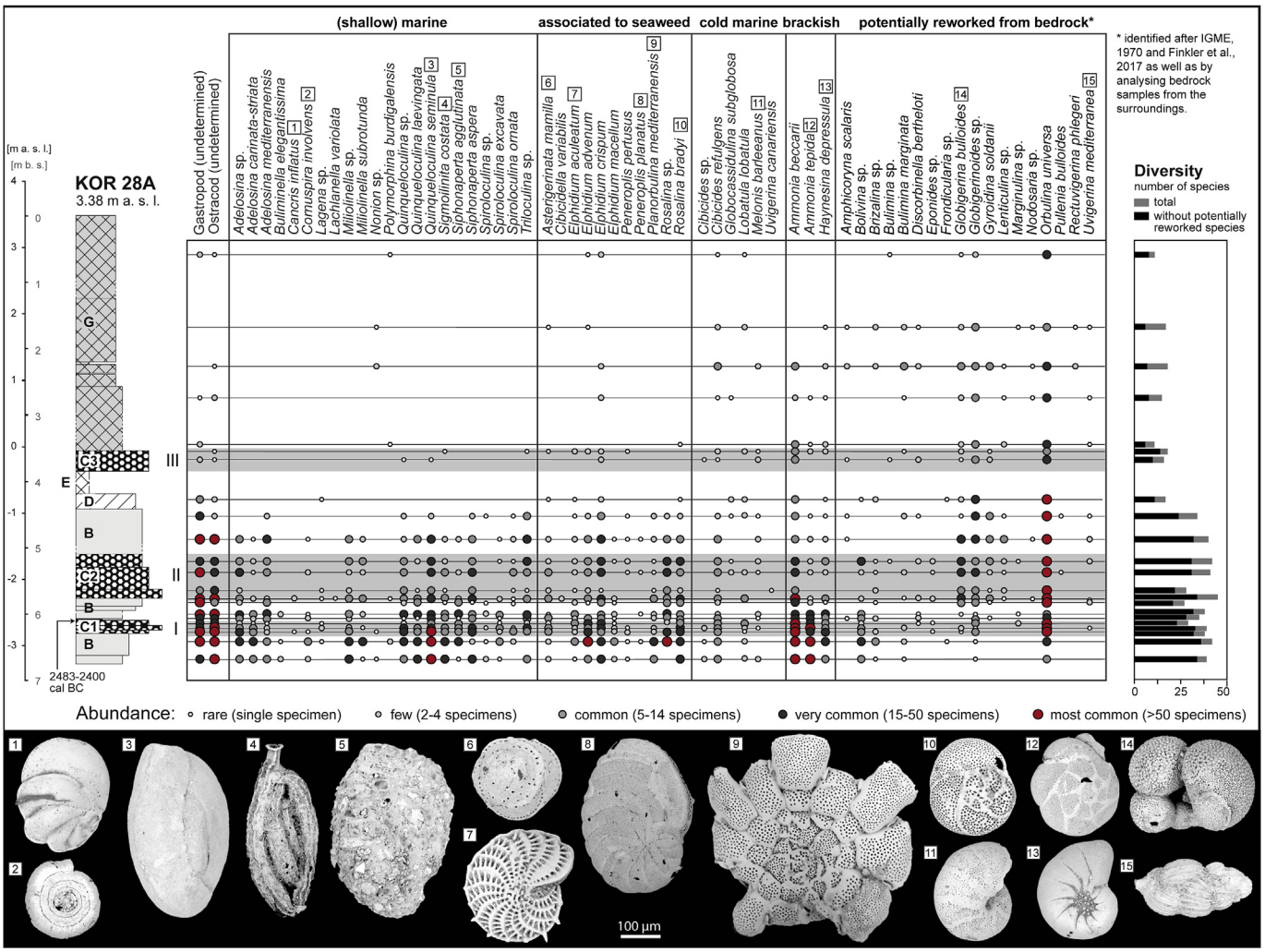

Fig. 6. Results of microfaunal analyses for samples from vibracore KOR 28A based on a semi-quantitative approach. Species are classified according to their ecological preferences after Murray (2006) and Sen Gupta (1999). Potentially reworked species from the Neogene bedrock were identified after IGME (1970), Finkler et al. (2017) and by analysing bedrock samples from the surroundings. Shallow marine sands show decreasing diversity and abundance of foraminifera towards the top. The two high-energy event layers found in the lower part of the core are similar to shallow marine sediments regarding their microfaunal content. In contrast, high-energy deposits found on top of the ramp are characterised by lower abundance and diversity.

high-energy inundation from the sea side.

Units D and E were retrieved from vibracore KOR 28A and occurred in a stratigraphical position consistent with the harbour deposits encountered at site KOR 37A. Due to the position of coring site KOR 28A, approximately in the midst of the Pierri site ramp, we interpret the stone layer (E) and the underlying homogeneous fine sands (D) as ***anthropogenic***, brought in by man and being probably the artificial base of a ramp.

In contrast to unit B, unit F is characterised by ***lagoonal*** conditions, represented by the entry of silt associated with slightly decreased marine indicators. Moreover, the foraminifers *Planorbulina mediterranea* and *Peneroplis* sp. were found, both related to *Posidonia*, that indicate quiet and shallow water conditions (Murray, 2006). Salinity most likely changed towards brackish conditions to the top of the unit. This is mirrored by decreased diversity of species and the dominance of *Ammonia* which is one of a few genera tolerant towards brackish waters. Unit F deposits were found right in front of and associated with archaeological remains of the Pierri quay wall so that we interpret them as ***harbour deposits***. Our data further show that this harbour environment was subject to Pb pollution indicating intense use of Pb as ballast for ships and working material. Pb is one of the first metals used by man (Lessler, 1988) with a very low natural background signal. Therefore, extensive occurrence of Pb is strongly linked to mining and metallurgy (Hong et al., 1994; Brännvall et al., 2001) and acts as an excellent tracer for human activities (Marriner and Morhange, 2007). Pb pollution reaches its highest level during Roman times causing considerable Pb accumulations in ancient harbour basins (e.g. Le Roux et al., 2003, 2005; Véron et al., 2006; Elmaleh et al., 2012; Delile et al., 2014; Hadler et al., 2013, 2015; Stock et al., 2016).

Unit G, forming the uppermost part of all cores, contains a high amount of cultural debris and ceramic sherds, embedded in a silty matrix. Its brown colour documents weathering processes and pedogenesis. Findings of reworked planktonic and cold-marine species indicate erosion from the adjoining hillslopes of the Analipsis Ridge. Unit G thus represents post-harbour ***colluvial to anthropogenic*** sediments.

5.2. High-energy impacts on the harbour site

In the following, we will discuss potential causes for the deposition of the specific high-energy deposits that were found in

Please cite this article in press as: Finkler, C., et al., Geoarchaeological investigations of a prominent quay wall in ancient Corcyra – Implications for harbour development, palaeoenvironmental changes and tectonic geomorphology of Corfu Island (Ionian Islands, Greece), Quaternary International (2017), http://dx.doi.org/10.1016/j.quaint.2017.05.013

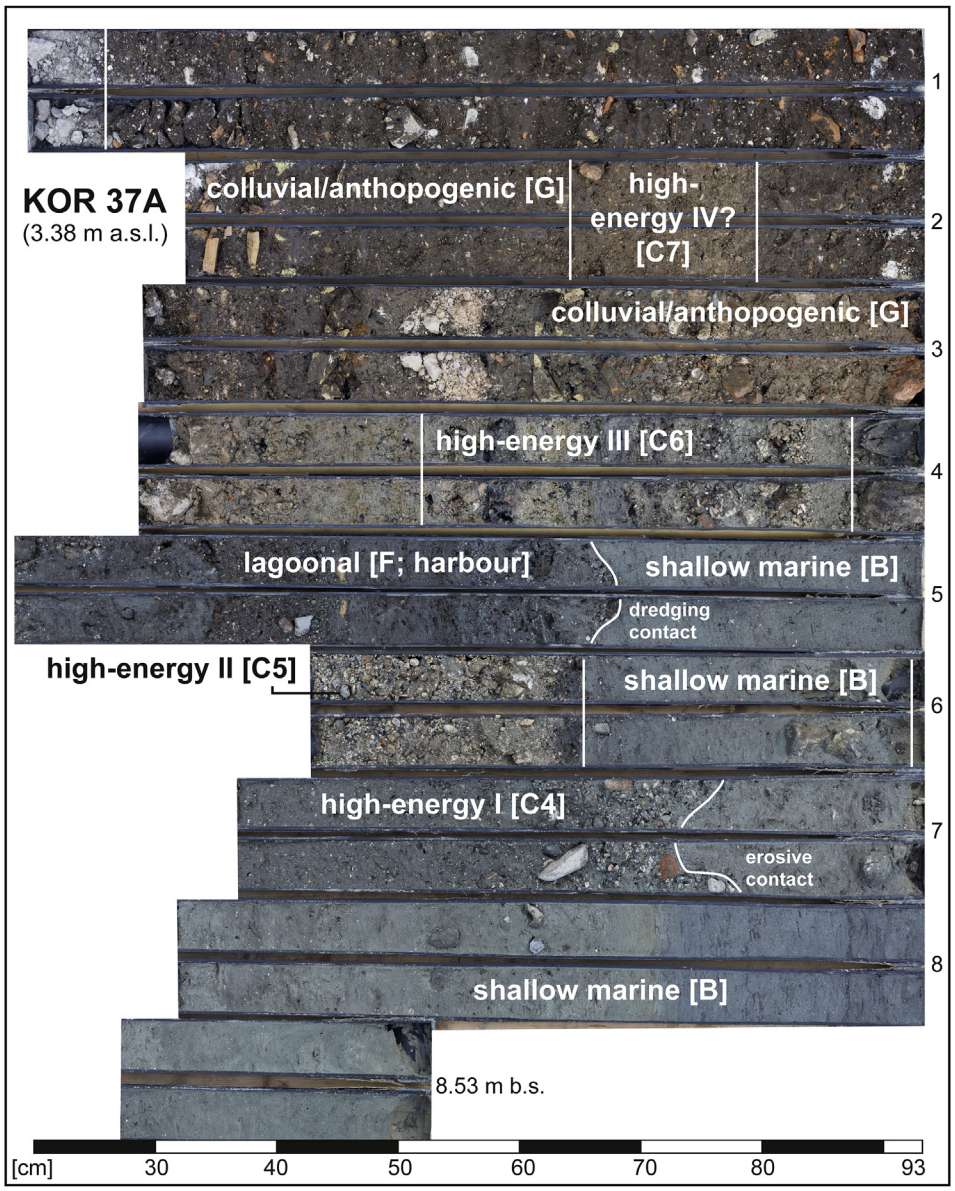

Fig. 7. Stratigraphical record of vibracore KOR 37A. Shallow marine sands show intersected high-energy layers and are followed by thick colluvial to anthropogenic deposits. Harbour deposits (4.63–4.17 m b.s.) are characterised by an abrupt increase of silt content and contain stones, ceramic fragments and organic material. Capital letters B–G represent associated stratigraphical units described in the results chapter.

vibracores at the Pierri site.

First, slope erosion associated with torrential run-off from the adjoining Analipsis Ridge can be easily excluded as potential trigger. The Pierri event layers (unit C) are not dominated by those foraminifera species that are typical of the local Neogene bedrock. They rather show a huge variation in species diversity (Figs. 6 and 9; Table 2) documenting the input of foraminifera from different Holocene marine environments. Thus, it is obvious that these layers are the result of extreme wave impact from the sea side that hit the Gulf of Corfu and the ancient harbour zone to the north of the Analipsis Peninsula. By these events, water masses intruded with high flow velocities and eroded, transported and strongly reworked autochthonous littoral and shallow marine sediments from the direct environs of the harbour bay and the adjacent gulf. These sediments with a mixed palaeoenvironmental signature were then deposited at the Pierri site. Based on the sedimentary record at Pierri, high-energy marine inundations are to be characterised as high magnitude-low frequency events. Extreme wave impact from the seaside is potentially caused by both, storms and tsunamis, and, in outer-Mediterranean regions, both phenomena show similar sedimentological effects (cf. Morton et al., 2007; Switzer and Jones, 2008; Lario et al., 2010); however, the forcing agents are completely different.

The northern Ionian Sea is characterised by a weak to medium wind and wave climate with mean significant wave heights of 1.2–1.6 m and very low annual wave energy flux (Cavaleri, 2005; Karathanasi et al., 2015). However, heavy storms may occasionally occur associated to cyclones of the west wind zone, sometimes related to so-called medicanes (Cavicchia et al., 2014). Such medicanes appear with a low frequency but are reported from the Ionian Sea by several authors (e.g. Davolio et al., 2009; Miglietta et al., 2015). They may generate extreme wave heights in the open sea such as offshore the Ionian Islands where Ghionis et al. (2015) measured significant wave heights of more than 5 m during a

Please cite this article in press as: Finkler, C., et al., Geoarchaeological investigations of a prominent quay wall in ancient Corcyra – Implications for harbour development, palaeoenvironmental changes and tectonic geomorphology of Corfu Island (Ionian Islands, Greece), Quaternary International (2017), http://dx.doi.org/10.1016/j.quaint.2017.05.013

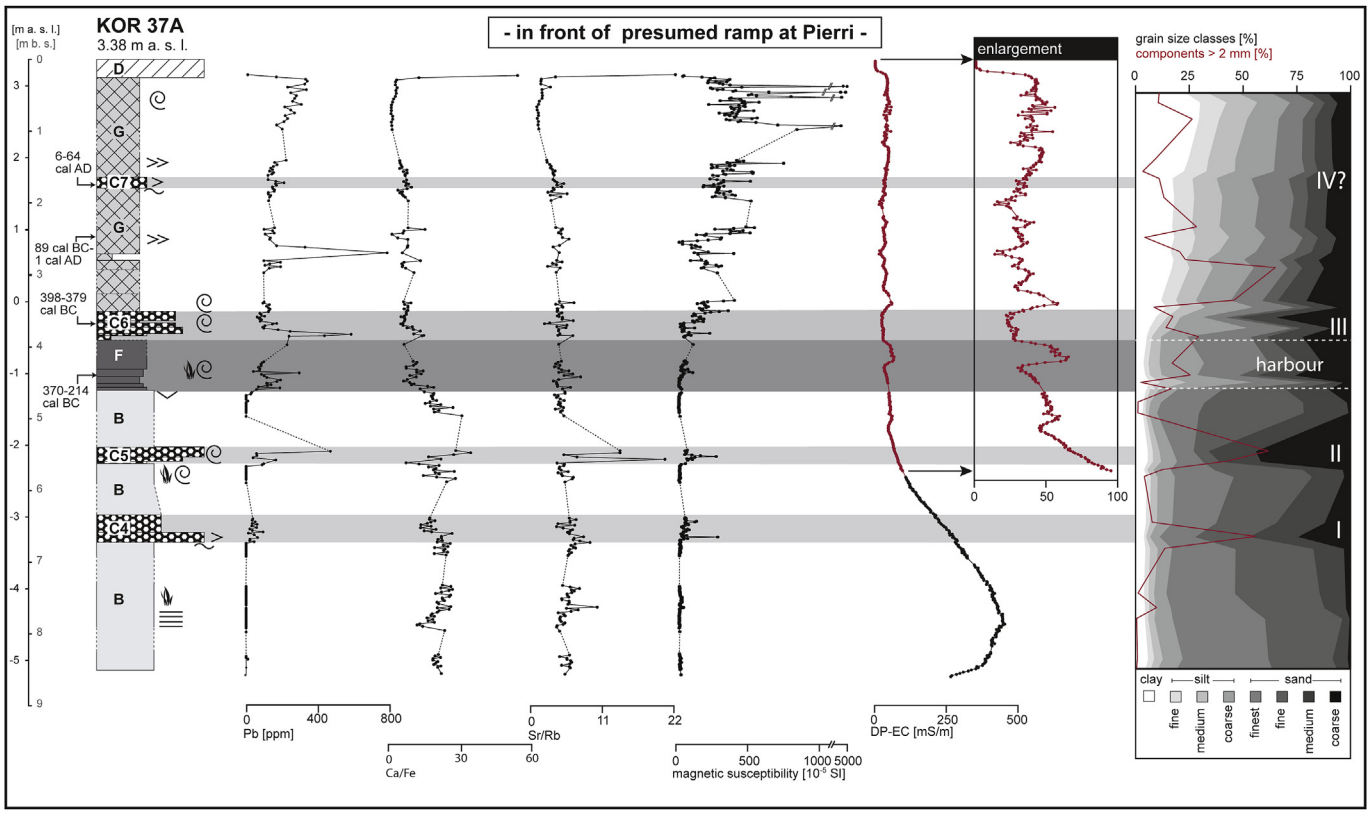

Fig. 8. Results of grain size analysis, magnetic susceptibility measurements, Direct Push EC logging and selected geochemical proxies for vibracore KOR 37A. High-energy layers are highlighted by light grey colour and are characterised by coarser grain size and distinct peaks of Pb concentration, magnetic susceptibility values and marine ratios. In contrast, silty harbour deposits on top of the shallow marine sands (dark grey) show strongly reduced marine influence (lower Ca/Fe values, finer grain size). Legend according to Fig. 5.

storm in 2007 only a few kilometres west of Corfu Island. The maximum observed storm wave height in the open Ionian Sea does, however, not exceed 6–7 m (Scicchitano et al., 2007). Nevertheless, such high waves are bound to open sea conditions and are strongly reduced when propagating towards the coasts by wave shoaling.

Moreover, local geographical and topographical conditions have to be taken into account. The Gulf of Corfu is a shallow marine indentation with a maximum width of 25 km and water depths not deeper than 70 m. It is connected to the open sea by narrow straits, namely the strait between Aghios Stefanos and Ksamil in the north and the strait between Syvota and Kavos in the south, 2 km and 8 km wide, respectively (Fig. 1B). The widely-travelled geographer Partsch (1887) described it as a lake-like embayment. It is extremely well protected from the rough waves of the open Ionian Sea and represents one of the best sheltered natural harbour settings of the eastern Mediterranean. In contrast, the open Ionian Sea west off Corfu shows a narrow shelf zone and water depths reaching 1000 m only few kilometers distant from the western coast of the island. Storm wave models reveal wave heights of more than 10 m for the open Ionian Sea whereas the Gulf of Corfu shows small wave heights of less than 1.5 m (Mazarakis et al., 2012; Zacharioudaki et al., 2015).

From these points of view, storms can be excluded as agents for repeated extreme wave impacts in the Gulf of Corfu as recorded at Pierri. Instead, earthquakes and tsunamis, which are both known to have repeatedly affected Corfu Island during history (Section 2.1), must be considered. Recent investigations on extreme event deposits found on the east coast of Corfu prove that both, teletsunamis and local tsunamis, for example triggered by submarine mass movements off the west coast of the island, may produce considerable tsunami waves in the Gulf of Corfu due to wave refraction and diffraction (Fischer et al., 2016a; Finkler et al., 2017). Furthermore, repeated tsunami landfall on Corfu is well documented in earthquake and tsunami catalogues (Partsch, 1887; Soloviev et al., 2000; Albini, 2004; Ambraseys and Synolakis, 2010).

Distinct sedimentological and geochemical features known from modern tsunami and palaeotsunami research were detected in high-energy subunits C1–C8. Amongst others, such features are (i) a sharp erosional contact towards the underlying autochthonous deposits due to high flow velocities (Fujiwara et al., 2000; Hawkes et al., 2007; Sakuna et al., 2012), (ii) silt-dominated rip up clasts due to reworking of finer grained underlying material (Goff et al., 2001; Gelfenbaum and Jaffe, 2003), (iii) fining upward sequences caused by varying and overall decreasing energy in the course of tsunami inundation (Shi et al., 1995; Hawkes et al., 2007; Sakuna et al., 2012), and (iv) the input of marine calcium carbonate in the form of shells and faunal tests (Goff et al., 2001; Fujiwara et al., 2000; Vött et al., 2011a, 2011b), entailing the increase in concentrations and distinct peaks of Ca, Sr, Ca/Fe and Sr/Rb, the latter including terrestrial elements like Fe or Rb (Mathes-Schmidt et al., 2013; Chagué-Goff et al., 2015; Vött et al., 2011a, 2011b, 2015). Finally, (v) breaks in the geochemical pattern indicate short-term abrupt, mostly temporary changes in the palaeoenvironmental conditions through the input of allochthonous sediments. For example, nearly all event layers encountered in the Pierri geoarchive show strongly increased Pb concentrations, whereas under- and overlying autochthonous sands are almost void of Pb. Increased Pb concentrations in event layers can be explained by the strong affection of Pb-polluted areas, such as harbours, by the inundation event and the consequent entrainment of polluted material further inland. Ancient harbours are known to be related with high Pb concentrations (e.g. Hadler et al., 2013) due to the overall use of Pb for

Please cite this article in press as: Finkler, C., et al., Geoarchaeological investigations of a prominent quay wall in ancient Corcyra – Implications for harbour development, palaeoenvironmental changes and tectonic geomorphology of Corfu Island (Ionian Islands, Greece), Quaternary International (2017), http://dx.doi.org/10.1016/j.quaint.2017.05.013

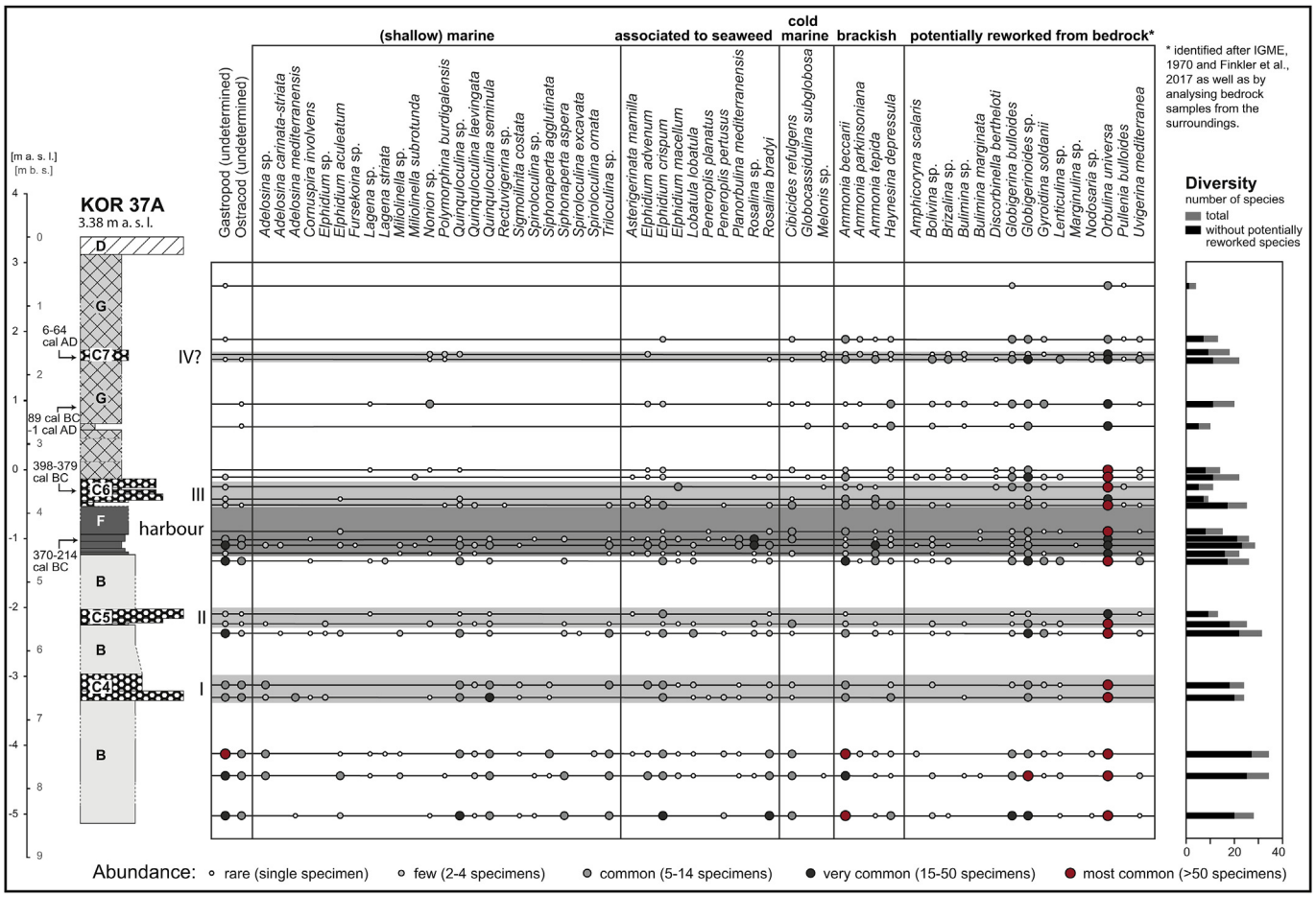

Fig. 9. Results of microfaunal analysis for selected samples from vibracore KOR 37A. Species are classified according to their ecological preferences after Murray (2006) and Sen Gupta (1999). Potentially reworked species from the Neogene bedrock were identified after IGME (1970), Finkler et al. (2017), and by analysing bedrock samples from the surroundings. The two lower high-energy layers (I, II) show a similar foraminiferal assemblage as the basal shallow marine sands, characterised by high diversity and high abundance. In contrast, diversity decreases in the upper part of the harbour sediments. Here, foraminifera tolerant to brackish conditions and species of shallow seaweed assemblages are dominating. This foraminiferal fingerprint mirrors a protected environment, probably shielded by a breakwater or similar constructions. High-energy layer III strongly resembles these harbour deposits while a potential high-energy IV differs from the over- and underlying colluvial sediments due to the input of marine and brackish fauna.

Table 1
Simplified local stratigraphic records of vibracores KOR 3, KOR 28A and KOR 37A

Vibracore	Depth [m b.s.]	Grain size	Colour	Characteristics	Unit
KOR 3	0.00–1.61	clayey silt	brownish	contains cultural debris	G
	1.61–2.35	gravel in sand matrix	brownish	contains ceramics	C8
	2.35–2.77	silt to silty sand	dark grey	contains organic material, peat to the top	F
	2.77–6.93	fine to finest sand	greyish	well sorted	B
	7.00–8.85	silty clay	grey	compact	A
KOR 28A	0.00–3.52	clayey silt	brownish	contains cultural debris	G
	3.52–3.87	coarse sand	greyish/brownish	contains ceramics	C3
	3.87–4.17	solid stone	white/yellowish	calcareous	E
	4.17–4.40	fine sand	light-grey	very homogeneous	D
	4.40–5.08	fine to finest sand	grey	well sorted, plant remains at the top	B
	5.08–5.75	gravel in sand matrix	multi-coloured	sharp basal contact, contains ceramics	C2
	6.75–6.06	fine to finest sand	grey	well sorted	B
	6.06–6.23	medium to coarse sand	grey	fining upward tendency	C1
	6.23–6.93	fine to finest sand	grey	well sorted	B
KOR 37A	0.00–1.64	clayey silt	brownish	contains cultural debris	G
	1.64–1.79	clayey silt	light brown	sharp basal contact	C7
	1.79–3.53	clayey silt	brownish	contains cultural debris	G
	3.87–3.53	gravel and sand	multi-coloured	contains ceramics	C6
	4.17–4.63	silt to silty sand	dark grey	sharp basal contact, poorly sorted	F
	4.63–5.42	fine to finest sand	grey	well sorted	B
	5.42–5.65	gravel in sand matrix	brownish/multi-coloured	heterogeneous	C5
	5.65–5.93	fine to finest sand	grey	well sorted	B
	6.36–6.75	fine to coarse sand	grey	sharp basal contact, contains ceramics	C4
	6.75–8.53	fine to finest sand	grey	well sorted	B

Please cite this article in press as: Finkler, C., et al., Geoarchaeological investigations of a prominent quay wall in ancient Corcyra – Implications for harbour development, palaeoenvironmental changes and tectonic geomorphology of Corfu Island (Ionian Islands, Greece), Quaternary International (2017), http://dx.doi.org/10.1016/j.quaint.2017.05.013

Table 2
Sedimentary, geochemical and palaeontological features of high-energy layers (subunits C1–C8) detected in the Pierri site sedimentary record (vibracores KOR 3, KOR 28A, KOR 37A). Foraminiferal fingerprints were classified according to Figs. 6 and 9.

	vibracore	KOR 28A			KOR 37A				KOR 3
	subunit	C1	C2	C3	C4	C5	C6	C7	C8
Sedimentary features	multimodal grain size distribution	+	+	+	+	+	+	+	+
	erosional basal contact	−	+	−	+	+	o	+	+
	fining upward tendency	+	+	−	+	+	+	−	−
	bad sorting	+	+	+	+	+	+	+	+
	mup cap	+	−	−	−	−	−	−	−
	rip-up clasts	−	+	−	−	−	−	−	−
	embedded gravel	+	+	+	+	+	+	−	+
	embedded ceramic sherds	−	+	+	+	−	+	+	+
geochemical signals	increased marine ratios	+	+	−	−	+	−	−	o
	increased Pb values	−	+	+	+	+	+	−	o
	increased magnetic susceptibility	−	+	+	+	+	+	−	o
	decreased LOI values	o	o	o	o	o	o	o	+
palaeontological features	marine macrofauna	+	+	+	−	+	+	−	−
	shell debris	+	+	−	−	−	−	−	−
	Foraminifera fingerprint	B	B	F	B	B	F	mixed	o
event chronology		I	II	III	I	II	II	IV?	III

Explanations: + = feature existent; − = feature absent; o = no data available; B = shallow marine; F = lagoonal.

stabilizing ships and to join quay ashlars by Pb clamps. Abrupt changes of geochemical proxies are typically related to temporary high-energy impact. As, for the Pierri site, the influence of both severe storms and torrential runoff is excluded, we interpret high-energy event layers found at Pierri as the results of tsunami landfall.

On a small scale, high-energy sediments trapped in the Pierri record show different characteristics (Table 2) and can be grouped into four tsunami event layers (I to IV). Subunits C1 and C4 are located in consistent stratigraphical positions and are thus classified as ***high-energy layer I***; both show distinctly increased multimodal grain size, a general fining upward tendency and bad sorting. Their microfaunal signature mostly mirrors the shallow marine signal of local near-coast environments. We conclude that by tsunami flooding autochthonous near-coast littoral deposits were eroded, reworked and transported over a short distance (cf. Goff et al., 2001; Bahlburg and Weiss, 2007; Hawkes et al., 2007). Yet, subunit C1 seems to have been subject to already slightly reduced flow velocities and wave energy, resulting in a missing erosional contact, smaller grain size when compared to subunit C4 as well as the presence of a mud cap on top (Fig. 4B). Increased Pb values in the event layer in KOR 37A might be caused by early Bronze Age human influence the presence of whom is shown by embedded ceramic sherds.

High-energy layer II (subunits C2 and C5) is also made out of near-coast littoral material. Both subunits show nearly identical features (Table 2), even if grain size in subunit C5 (KOR 37A) is characterised by coarser clasts and embedded ceramic sherds similar to subunit C4.

Both high-energy layers I and II could not be identified macroscopically within the sedimentary record of vibracore KOR 3. However, grain size distribution reveals two minor peaks in the amounts of medium and coarse sand (Fig. 5), which might be related to the impact of tsunami events I and II.

In contrast to high-energy layers I and II, subunits C3/C6 and C8 are not embedded in shallow marine sands but are located on top of harbour sediments or a ramp structure, respectively. The foraminiferal fingerprint of this ***high-energy layer III*** reflects reworking of lagoon-type harbour sediments which were obviously primarily eroded and reworked in the course of the event. Apart from that, the sedimentary subunits show similar features (Table 2).

Finally, a ***potential event layer IV*** (C7) was found in the record of vibracore KOR 37A. As the layer lies on top of thick colluvial/anthropogenic deposits, the Pierri site was already solid ground when these sediments were deposited. However, the geochemical and microfaunal fingerprint of this potential high-energy layer differs slightly from the under- and overlying colluvial/anthropogenic deposits. Still, potential extreme wave impact is mirrored by slightly increased grain size and few marine to brackish species which occur next to potentially reworked species of colluvial origin.

We conclude that high-energy layers encountered in vibracores at the Pierri site were deposited within the course of multiple tsunami landfalls. Three events occurred when the Pierri site was still dominated by shallow marine (events I and II) or lagoon-type harbour conditions (event III). Another impact (event IV), the traces of which are weaker than those recognized for events I to III, may potentially be related to tsunami landfall when the Pierri harbour zone was already dry land.

5.3. Dating approach, marine reservoir effect and relative sea level indicators

We established a geochronostratigraphical frame for the Pierri site based on five ^{14}C AMS samples out of organic material which were extracted from vibracores KOR 28A and KOR 37A (Table 3). These dates are supplemented by radiocarbon ages of three oyster samples collected from the Pierri quay wall segment (Fig. 10C) and additional two radiocarbon dates from the close proximity (Finkler et al., 2017), providing information on relative sea level changes (Table 3). In addition, archaeological age estimates of seven ceramic fragments were used to cross-check radiometric ages (Table 4).

Calibration of radiocarbon ages was performed by means of the software Calib 7.1 (Stuiver and Reimer, 1993; Reimer et al., 2013). However, even when calibrated, radiocarbon dates only yield approximate time frames and no exact dates, as inaccuracies caused by long term variations within the production of atmospheric ^{14}C, isotopic fractionation, contamination or relocation of sample material may occur (Geyh, 2005; Walker, 2005). The latter is especially true for samples retrieved from high-energy layers, as high-energy events usually erode and rework older deposits (Goff et al., 2001). This erosion can also produce considerable hiatuses. For this reasons, the sandwich-dating technique using both, a *terminus ante quem* (before) and a *terminus post quem* (after) for the event is the best appropriate manner to date high-energy layers. Unfortunately, sandwich-dating was not possible in this study, as there was no datable material available below and above the encountered high-energy deposits. Therefore, three samples were

Please cite this article in press as: Finkler, C., et al., Geoarchaeological investigations of a prominent quay wall in ancient Corcyra – Implications for harbour development, palaeoenvironmental changes and tectonic geomorphology of Corfu Island (Ionian Islands, Greece), Quaternary International (2017), http://dx.doi.org/10.1016/j.quaint.2017.05.013

Table 3
Radiocarbon dating results of samples from vibracores drilled at the Pierri sites and from the oyster band adhesive to the Pierri quay wall.

Sample ID	Depth [m b.s.]	Depth [m a.s.l.]	Sample material	Lab. No.	$\delta^{13}C$ [ppm]	^{14}C age [BP]	2σ age [cal BC/AD]	1σ age [cal BC/AD]
KOR 28A/PR 3	6.07	−2.59	seaweed	MAMS 24902	−18.3 [a]	4276 ± 23	2539–2347 BC	2483–2400 BC
KOR 37A/HK 2	1.75	1.63	charcoal	MAMS 24912	−34.4	1968 ± 25	38; 78 AD	6–64 AD
KOR 37A/HK 3	2.47	0.91	charcoal	MAMS 24913	−35.0	2040 ± 24	156 BC; 23 AD	89 BC; 1 AD
KOR 37A/HK 10	3.69	−0.31	charcoal	MAMS 24911	−28.8	2301 ± 22	404; 262 BC	398–379 BC
KOR 37A/HR 0	4.39	−1.01	wood	MAMS 24914	−29.6	2236 ± 23	370; 214 BC	383; 207 BC
KOR Pierri Tx16 L1	–	−0.21	oyster	MAMS 29601	2.4 [a]	2511 ± 23	336–154 BC	293–183 BC
KOR Pierri Tx16 M2	–	−0.17	oyster	MAMS 29602	1.3 [a]	2550 ± 24	354–191 BC	335–235 BC
KOR Pierri Tx16 U3	–	−0.03	oyster	MAMS 29603	2.0 [a]	2517 ± 23	339–161 BC	298–191 BC
KOR 1A/HK 9+ [c]	2.65	−0.99	charcoal	UCI 121509	[b]	1600 ± 25	404–536 AD	413; 536 AD
KOR 5/32+ HR [c]	9.81	−8.51	peat	MAMS 19770	−27.4	7328 ± 28	6238–6089 BC	6232; 6140 BC

Note: b.s. – below ground surface. a.s.l. – above sea level. MAMS – Klaus-Tschira Laboratory of the Curt-Engelhorn-Centre Archaeometry gGmbH Mannheim, Germany. UCI – Keck Carbon Cycle AMS Facility, University of California at Irvine, USA. 1σ/2σ age –calibrated ages, 1σ/2σ range. ";"– several possible age intervals due to multiple intersections with the calibration curve. All dates are calibrated using Calib 7.1 (Stuiver and Reimer, 1993; Reimer et al., 2013).

[a] – marine sample, calibrated by using the marine13 calibration dataset with an average reservoir age of 405 years.

[b] – ^{13}C correction is done automatically with a standard run.

[c] – published in Finkler et al. (2017).

extracted from high-energy layers themselves. The resulting ages must be considered as *termini ad* or *post quos*, thus mere maximum ages.

Radiocarbon data of the Pierri site (Table 3) result in a consistent age model reaching from the 3rd millennium BC to the 1st cent. AD and correlate well with archaeological ages estimates of diagnostic ceramic fragments (Table 4). Only sample KOR 37A/HK 1 produces an age-inversion of some decades when compared to sample KOR 37A/HR 0. As this sample was extracted from a high-every layer, the slight inversion is most likely caused by reworking effects.

Radiocarbon dating of samples out of marine material is problematic as oceans function as large carbon reservoirs, resulting in significantly older ages compared to contemporaneous terrestrial material. Marine calibration requires the correction of the local reservoir age of the environment where the particular samples were taken from (e.g. Reimer and McCormac, 2002). This marine reservoir effect (MRE) is, however, subject to variations in space (different MRE for different environmental settings), time (MRE

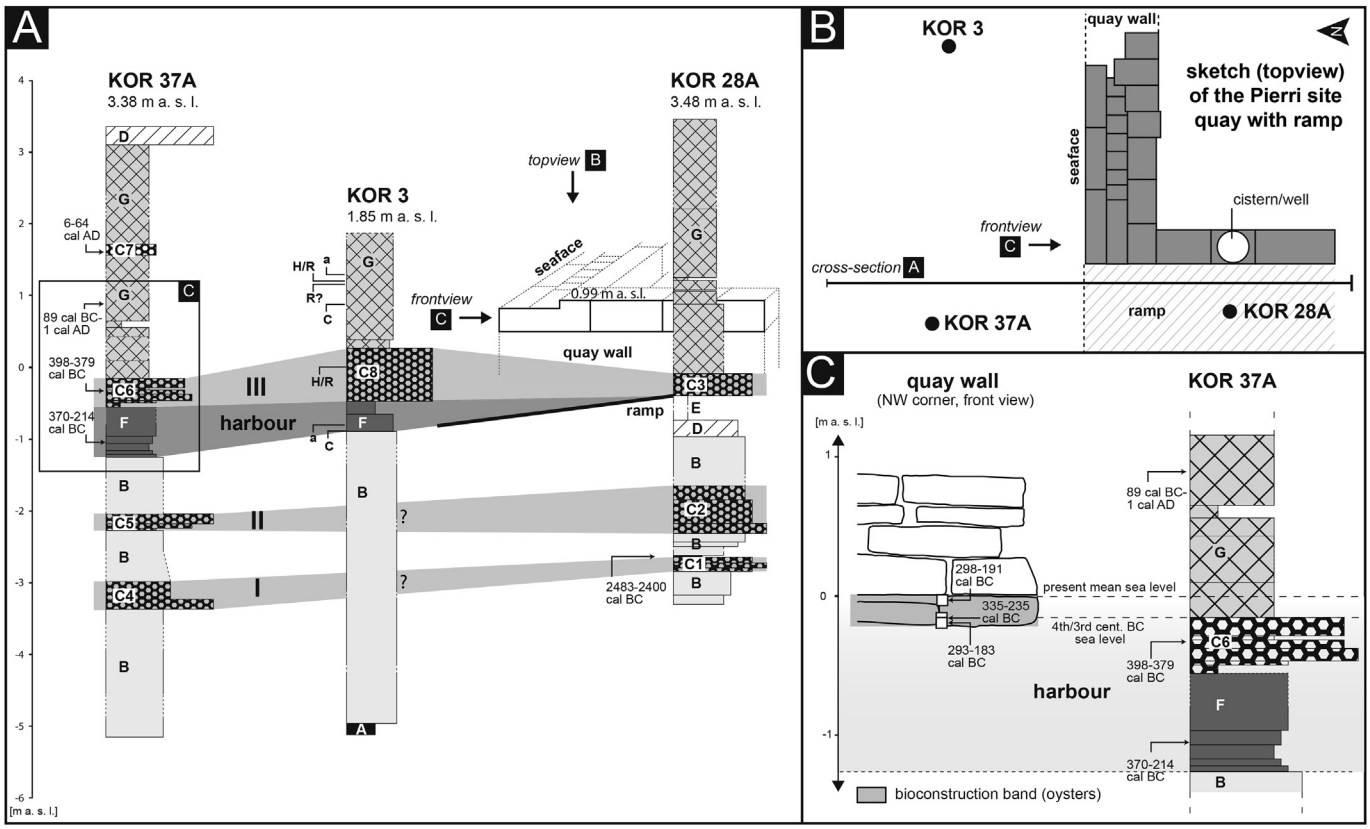

Fig. 10. (A) Cross-section of all vibracores retrieved at the Pierri site with simplified facies pattern and ^{14}C ages. Note the location of the Pierri quay wall (only true to scale in vertical direction) with associated harbour sediments and ramp. (B) Simplified sketch (top view) of the Pierri site quay and locations of the vibracores depicted in A. (C) Sketch of the northwestern corner of the quay wall segment (front view) compared to the associated stratigraphy of vibracore KOR 37A (please see A for detailed section). Oyster bioconstruction band adhesive to the lower Pierri quay wall ashlar is depicted by grey colour, oyster samples that were radiocarbon dated are marked by white rectangles. The overall time span when oysters were alive was found to be 335-183 cal BC which is in accordance with the archaeological age of the harbour, dated to Classical-Hellenistic times (Riginos et al., 2000). Legend according to Fig. 5.

Please cite this article in press as: Finkler, C., et al., Geoarchaeological investigations of a prominent quay wall in ancient Corcyra – Implications for harbour development, palaeoenvironmental changes and tectonic geomorphology of Corfu Island (Ionian Islands, Greece), Quaternary International (2017), http://dx.doi.org/10.1016/j.quaint.2017.05.013

Table 4
Archaeological age estimates for diagnostic ceramic fragments found in the vibracores drilled at the Pierri site.

Sample ID	Depth [m b.s.]	Depth [m a.s.l.]	Sample description	Age estimation
KOR 3/1+ K1	0.56	1.29	undetermined	ancient
KOR 3/2 K	0.65	1.20	fragment of *skyphos*	late 6th-5th cent. BC
KOR 3/2 K2	0.69	1.16	undetermined	Hellenistic or Roman
KOR 3/3 K	0.99	0.86	fragment of brick	Roman?
KOR 3/5+ K	1.85	0.00	fragment of cookware	Hellenistic or Roman
KOR 3/10 K	2.67	−0.82	undetermined	ancient
KOR 3/10+ K	2.74	−0.89	fragment of ceramics	Classical
KOR 37A/K1	2.68	0.7	undetermined	undetermined

variations through the Holocene) and species (different MRE for different species), even on a local to regional scale (Walker, 2005). As for most of the coastal regions worldwide, these regional to local variations of the MRE are unknown for Corfu, so that we used the global marine13 dataset with an average reservoir correction of 405 years (Reimer et al., 2013) to guarantee comparability.

Sample KOR 28A/PR3 was identified as marine sample due to a δ^{13}C-value of −18.3 ppm (Table 3; Walker, 2005). Its calibrated age must therefore be treated with caution, as the real MRE is not known.

Additionally, a band of marine bioconstruction including abundant oyster shells was found adhered to ashlars that belong to the foundation level of the Pierri quay wall (see Sections 5.4 and 5.5 and Figs. 10 and 12). This bioconstruction band mirrors the approximate relative sea level in the Pierri harbour basin for the time when it was in use. In order to obtain a reliable age determination of this important geoarchaeological sea level indicator, oyster samples were taken from the upper and lower edges of the bioconstruction band as well as from in between, namely samples KOR Pierri Tx16 L1, KOR Pierri Tx16 U3 and KOR Pierri Tx16 M2, respectively. The three samples yielded radiocarbon ages that are identical within the range of errors, in particular 293–183 cal BC, 298–191 cal BC and 335–235 cal BC, respectively (1σ intervals, see Table 3). Thus, the entire time period spanned by the three oyster samples is 335–183 cal BC. These results are in perfect accordance with the archaeological age of the Pierri harbour dated to the Classical-Hellenistic Period (Riginos et al., 2000). Moreover, they fit well with the age of the terrestrial wooden radiocarbon sample KOR 37A/HR 0, dated to 370–214 cal BC (see Table 3) and the archaeological age of the diagnostic ceramic fragment KOR 3/10+ K, dated to Classical times (see Table 4 and Sections 5.4 and 5.5).

From a methodological point of view, the calibrated age of the bioconstruction band corroborates that the local MRE is, indeed, very well approximated with the average reservoir age of 405 years (Reimer et al., 2013) suggested within this study. If based on the non-marine calibration curve intcal13, oyster samples KOR Pierri Tx16 L1, KOR Pierri Tx16 U3 and KOR Pierri Tx16 M2 would yield 771–561 cal BC, 775–566 cal BC and 796–672 cal BC, respectively (1σ intervals, see Table 3), resulting in a total time span of 796–561 cal BC. Compared with the in situ sample KOR 37A/HR 0 that reflects the time when the harbour was in use and was dated to 370–214 cal BC (see Table 3), the age of the oyster band with MRE unconsidered would be 426–347 years too young. However, this MRE estimation is only valid for the Pierri oysters of this particular time frame and environmental setting.

Also, sample KOR 5/32+ HR represents a reliable indicator of local relative sea level during the mid-Holocene as it was extracted from a paralic peat layer. Sample KOR 1A/HK 9+ (terrestrial) roughly indicates the approximate relative sea level during early medieval times; it was taken from a section a few centimetres above a peat layer that was associated to the sea level at that time (Finkler et al., 2017).

5.4. Palaeogeographical evolution of the northern harbour zone in the environs of the Pierri site

Using a multi-proxy based approach, we were able to decipher the palaeoenvironmental evolution of the harbour environment associated with the Pierri site harbour facilities (Fig. 10A).

All vibracores drilled in the study area show shallow marine conditions at the base or right above the Neogene bedrock. These shallow marine sands are associated to an open marine inner shelf-environment with normal marine salinity and temperate to high water temperature (Murray, 2006; Figs. 6 and 9). Radiocarbon sample KOR 28A/PR 3 (Table 3), recovered from in situ shallow marine sands, implies that this system was already established before 2483–2400 cal BC. Besides, basal homogeneous sands were interrupted by two high-energy event layers (see chapter 5.5). By the establishment of the Pierri harbour and evidenced by local harbour sediments, a clear change from pre-harbour sand-dominated mid-energy open shallow marine conditions to a protected mid-to low-energy quiescent water body took place, the latter represented by silty grain size. Sample KOR 37A/HR 0 from the lower part of the harbour sediments yielded a radiocarbon age of 370–214 cal BC (Table 3). As a result, the harbour basin in front of the quay wall seems to have been in use during Classical to Hellenistic times. This is in accordance with the approximate age of the Pierri quay wall itself which was dated by the excavators to the Classical-Hellenistic period (Riginos et al., 2000).

The KOR 3 harbour sequence can be directly dated based on a diagnostic ceramic fragment dating to the Classical period. Here, increased amounts of silt and high amounts of organic material also document reduced wave dynamics. In contrast, the contemporaneous harbour sequence retrieved from vibracore KOR 37A is more heterogeneous and comprises fine and medium sand and even coarser clasts, maybe due to material input from the nearby Pierri quay wall.

The Pierri vibracore records neatly show that the harbour was developed out of an open shallow marine environment, most probably by the construction of breakwaters and associated harbour infrastructure that triggered a change from mid- to low-energy conditions at the site. However, the harbour architecture needed to create a protected harbour basin has to be clarified by detailed archaeological research. The KOR 37A harbour deposits sit right on top of a sharp contact in shallow marine fine sands which we interpret as evidence of a man-made excavation of the harbour basin or later dredging activities. Within the upper part of the harbour sediments, microfaunal analyses revealed an alteration of salinity towards more brackish conditions caused by the abrupt man-made protection of the environment, possibly in the form of breakwaters or other protective harbour facilities (Figs. 6 and 9). Additionally, vibracore 37A revealed decreasing Ca/Fe values due to an increase in terrestrial input of Fe.

During the time of its use, the harbour was hit by high-energy event III as documented by the coarse-grained subunits C3, C6

Please cite this article in press as: Finkler, C., et al., Geoarchaeological investigations of a prominent quay wall in ancient Corcyra – Implications for harbour development, palaeoenvironmental changes and tectonic geomorphology of Corfu Island (Ionian Islands, Greece), Quaternary International (2017), http://dx.doi.org/10.1016/j.quaint.2017.05.013

and C8 encountered in consistent depths in vibracores KOR 3, KOR 28A and KOR 37A. A piece of reworked charcoal retrieved from event layer III yielded a radiocarbon age of 398–379 cal BC. Another age is provided by a diagnostic ceramic fragment found in a consistent stratigraphical position in vibracore KOR 3 dating to Hellenistic to Roman times. Vibracores KOR 28A and KOR 37A show that the Pierri site was strongly hit by this event and subsequently lost its function as a harbour.

Finally, the harbour site was covered by colluvial to anthropogenic deposits during the 1st cent. BC and the 1st cent. AD as documented by radiocarbon samples from vibracore KOR 37A (Fig. 10A). This time window encloses the destruction of Corcyra by Roman troops in 31 BC so that the colluvial deposits encountered in up-core position of cores KOR 28A and KOR 37A possibly represent the associated destruction layer. The potential high-energy layer IV insects these colluvial to anthropogenic deposits in vibracore KOR 37A, suggesting that the area was possibly hit by another high-energy impact when the Pierri harbour was already silted up.

Although the harbour sequence recorded in vibracore KOR 37A starts in the 4th cent. BC only, it cannot be excluded that the Pierri site was already used as a harbour from the beginning of the Corcyrian seafaring activities from the Archaic period (8th cent. BC) onwards. The sharp dredging contact in vibracore KOR 37A may indicate a hiatus in the early harbour record concealing the harbour's history between Archaic and Classical times.

5.5. Archaeoseismological and tectonic implications of the Pierri record

Results from the Pierri site allow to draw conclusions with respect to the general palaeoseismological and tectonic history of Corfu Island, including (i) the establishment of a tsunami event chronology as well as (ii) the reconstruction of local co-seismic movements in space and (iii) of relative sea level fluctuations.

At least three tsunami events hit the eastern coast of Corfu, when shallow marine or lagoon-type harbour conditions prevailed at the Pierri site. Tsunami event I occurred before 2483–2400 cal BC as sample KOR 28A/PR 3 provides a minimum age for this event. The associated high-energy layer was found in consistent stratigraphical positions in cores KOR 30A, KOR 37A and KOR 28A (Fig. 10A).

Traces of tsunami event II were found in vibracores KOR 28A and KOR 37A again in stratigraphically consistent positions. Its geochemical fingerprint comprises considerable concentrations of Pb. This indicates that early harbour installations of the Helladic period, where Pb was ubiquitously used, were affected by this impact. Instead, Pb was not found in deposits of natural marine environments. Dating of event II is difficult because radiometric ages are not available. Yet, it must have taken place after 2483–2400 cal BC and before 370–214 cal BC taking ages of older and younger units in vibracore stratigraphies KOR 28A and KOR 37A, respectively, into consideration.

Tsunami event III can be dated as younger than 398–379 cal BC (reworked) and even younger than 370–214 cal BC based on the geochronostratigraphy available for vibracore KOR 37A (Fig. 10A). Event III deposits are lying right on top of the presumed Pierri ramp, the approximate age of which is dated to the Classical-Hellenistic period. Also, a diagnostic sherd dating to Hellenistic to Roman times was found in between event III deposits at site KOR 3. Finally, vibracore KOR 37A yielded a *terminus ante quem* of 89 cal BC to 1 cal AD for event III.

Traces of a possible event IV were detected in vibracore KOR 37A intersecting colluvial deposits. As this is a singular finding and there are no layers in consistent stratigraphical positions at neighbouring coring sites, tsunami origin of this layer is questionable. Its maximum age is dating to the 1st cent. AD.

Overall, these results correlate well with geomorphological and archaeoseismological studies conducted in western Greece along the shores of the eastern Ionian Sea and on Corfu Island itself. Event I can be correlated with an event of supra-regional dimensions described from various sites in western Greece dating to the early 3rd millennium BC (Vött et al., 2011b, 2015). Event II may possibly be related to a strong event around 1000 cal BC which has produced considerable local crust uplift on Corfu Island (Mastronuzzi et al., 2014) and for which tsunami traces were reported from different geological archives of Lefkada Island and the adjacent Greek mainland (Vött et al., 2006, 2009). If of tsunami origin, event candidate IV can be related to tsunami deposits found in the Roman phase of the Alkinoos Harbour dating to the 4th cent. AD (Finkler et al., 2017), most likely associated with teletsunami effects of the 365 AD tsunami. Traces of the 365 AD event, which was caused by a strong earthquake along a fault system offshore western Crete, are reported from southern Italy (e.g. De Martini et al., 2003; Mastronuzzi and Sansò, 2012), but also from the Sound of Lefkada and adjacent mainland Greece (Vött et al., 2009; May et al., 2012). Remains of Roman buildings from the 2nd to 3rd cent. AD in proximity to the Pierri quay wall (Morgan, 2010) document that the Pierri harbour site was solid ground already in the early 1st millennium AD. We conclude that events I, II and IV were triggered by supra-regional tsunamis that affected the Gulf of Corfu in the form of teletsunamis (see Finkler et al., 2017; Fischer et al., 2016a).

Most interesting conclusions can be drawn for event III. Pirazzoli et al. (1994) and Mastronuzzi et al. (2014) found evidence of a period of strong co-seismic uplift for the same time period, namely after 790–400 cal BC and after the 5th–4th cent. BC, respectively. We dated event III at Pierri to the time between the 4th and 1st cent. BC so that it may be hypothesised that it was caused by the earthquake that also triggered co-seismic uplift on the island as reported by Pirazzoli et al. (1994) and Mastronuzzi et al. (2014). This hypothesis is supported by archaeoseismological findings and sedimentological traces of tectonically induced crust movements:

Firstly, there is evidence from the side of archaeology, in particular from the monumental Hera temple on top of the Analipsis Peninsula (Fig. 2A), one of the earliest major temples in Greece built in c. 610 BC. Most of its architectural features date to late Classical or early Hellenistic times (Sapirstein, 2012). Earthquake-induced destruction of the temple and, above all, of its northern retaining wall can be seen since detailed excavations have started in 2012. Amongst others, the retaining wall shows abundant and clear archaeoseismological traces that document final destruction of the building by an earthquake, such as toppled ashlars and triangle-shaped corner break-outs (Fig. 11).

Secondly, archaeoseismological traces of seismically induced destruction between Classical and Hellenistic times were detected in the frame of a rescue excavation on the eastern shore of the Chalikiopoulou Lagoon in 2012 (Fig. 2A). Here, the Classical foundation of a building is covered by a thick layer of reworked lagoonal mud, containing sand, embedded allochthonous marine fauna, bones, ceramics and debris. On top of this destruction layer, the building was rebuilt in the Hellenistic period. Furthermore, parts of the excavated walls are strongly tilted, bearing witness of a strong and abrupt seismic impulse. The destruction layer described is consistent in age and stratigraphic position with event layer III found at Pierri and shows that tsunami landfall occurred all around the Analipsis Peninsula.

Thirdly, sedimentary evidence of co-seismic uplift is provided by the Pierri harbour deposits themselves. Harbour deposits of the Classical Pierri harbour complex were found at an elevation level of 1.25 m b.s.l. and higher. In contrast, the base of the younger Roman harbour mud, detected at the Kokotou site only 100 m to the west,

Please cite this article in press as: Finkler, C., et al., Geoarchaeological investigations of a prominent quay wall in ancient Corcyra – Implications for harbour development, palaeoenvironmental changes and tectonic geomorphology of Corfu Island (Ionian Islands, Greece), Quaternary International (2017), http://dx.doi.org/10.1016/j.quaint.2017.05.013

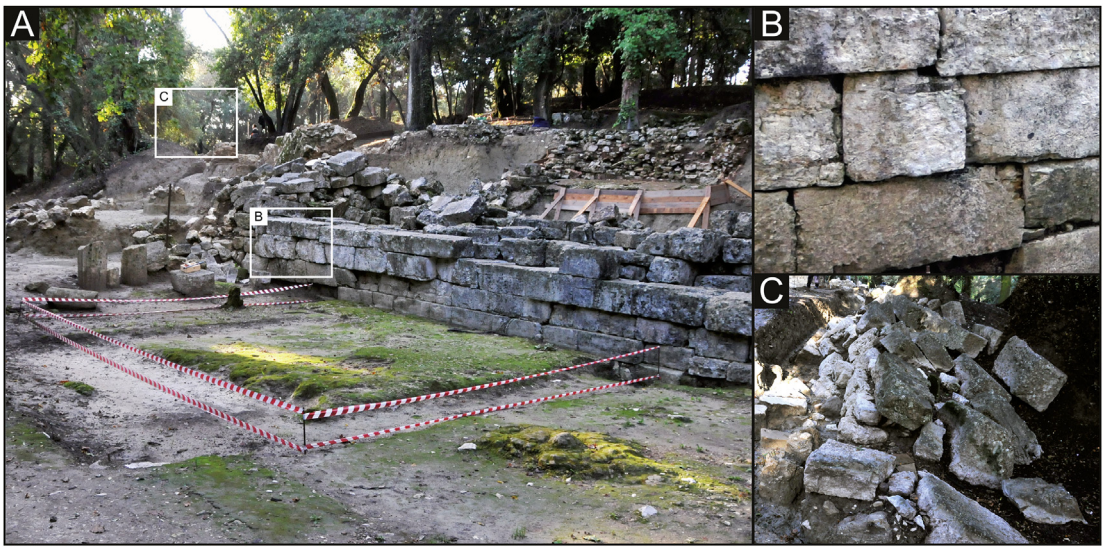

Fig. 11. Northern retaining wall of the temple of Hera showing typical archaeoseismological features, which indicate damage by an earthquake: (A) Parts of the wall have been shifted forward, (B) single ashlars show triangle-shaped corner breakouts and (C) large wall sections imply earthquake-related dislocation in a slopeward direction. (Photos by A. Vött, 2012).

was found at a distinctly lower elevation level of 3.40 m b.s.l. (Finkler et al., 2017). Obviously, the Classical harbour at Pierri was not navigable anymore in Roman times: it was uplifted what caused strongly decreased water depths within the remaining harbour. Associated to co-seismic uplift, caused by a local earthquake, tsunami waves hit the Pierri harbour leading to the deposition of corresponding event deposits (Fig. 12B). Traces of extensive dredging activities at the Kokotou site (Finkler et al., 2017) reflect the efforts to re-use at least the western part of the Classical harbour by dredging and deepening considerable parts of the former basin during Roman times (Fig. 12C). Regarding the exact timing of event III, the point in time when the oysters from the bioconstruction band found adhered to the Pierri quay wall died back between or right after 335–183 cal BC represents the best-fit age estimate for this event. The time span when oysters were alive was found to be maximum 335–183 cal BC which is in accordance with the archaeological age of the harbour, dated to Classical-Hellenistic times (Table 3; see Riginos et al., 2000).

Finally, we present an age-depth model of selected radiocarbon samples yielding information on relative sea level changes (Fig. 12E). During the mid-Holocene, the area was obviously dominated by tectonic subsidence as evidenced by sample KOR 5/32+ HR found at 8.51 m b.s.l. (Fig. 12E). The local age-depth relation given for this time period is consistent with age-depth relations recognized by Vött (2007) for the strongly subsiding coastal plains of Mytikas, Astakos and Boukka (Akarnania, northwestern mainland Greece; Fig. 12F). Our results are also in good accordance with the results of Marinos and Sakellariou-Mane (1964) who stated that subsidence on Corfu Island happened for the last time during the Neolithic era.

Fig. 12 further documents at least one abrupt change of the relative sea level (Fig. 12E): Marine oysters, spanning the time period 335–183 cal BC (see Section 5.3), were taken from an in situ bioconstruction band at the Pierri quay wall reflecting the relative sea level at the time when the harbour was in use. They are located on a distinctly higher elevation level compared to sample KOR 1A/HK 9+ dating to the 4th to 5th cent. AD. This sample was taken only 1 cm above a layer out of paralic peat that can be regarded at relative sea level indicator. Therefore, considerable co-seismic uplift must have occurred after Classical times, when the harbour had a stable water level and oysters colonised the quay wall, and before the 4th cent. AD. A second co-seismic movement, so far undated, as described by Pirazzoli et al. (1994) or even a yoyo-type fluctuation of the relative sea level as assumed by Mastronuzzi et al. (2014) are not reflected by the provided age-depth-model (Fig. 12E), most possibly due to the lack of appropriate dating material.

The earthquake-related destructions that were observed both at the Hera temple and associated to buildings at the eastern shore of the Chalikiopoulou Lagoon seem to have been caused by one and the same event. They can be dated, at both sites, to Classical-Hellenistic times. This date is consistent with the age of event layer III found at the Pierri site and with the dating of co-seismic uplift as recorded by the uplifted band of oysters, also at Pierri. We therefore suggest that the entire island was subject to strong earthquake influence at that time. This earthquake must have been caused by a local fault system, induced co-seismic uplift and triggered seismic sea waves that hit the east coast of Corfu. Considering radiocarbon dates and diagnostic ceramic fragments from the Pierri site as well as the dating of archaeoseismological traces described above, event III can be concisely dated to Classical to Hellenistic times, most probably to the 4th to 3rd cent. BC.

Beyond this aspect, important conclusions can be drawn with respect to the tectonic geomorphological development of the island. For the same time period, Pirazzoli et al. (1994) found co-seismically uplifted bio-erosional notches at the west coast of Corfu at an elevation of 1.6 m a.s.l. Even if the absolute amount of local co-seismic crust uplift at Pierri is not clear so far, we conclude that, here, the total uplift was clearly weaker compared to the west coast. In the east, the dated band of contemporaneous oysters at Pierri is located at 0.14 b.s.l. in average. Based on the vertical offset of c. 1.74 m, Corfu Island was not uplifted uniformly but rather asymmetrically; it was strongly tilted towards the east within the course of this local seismic event that occurred at a specific point in time during Classical to Hellenistic times.

6. Conclusions

Our study aimed to reconstruct the palaeoenvironmental setting in the environs of the prominent quay wall and presumed ramp structure at the Pierri site that are related to the northern harbour

Please cite this article in press as: Finkler, C., et al., Geoarchaeological investigations of a prominent quay wall in ancient Corcyra – Implications for harbour development, palaeoenvironmental changes and tectonic geomorphology of Corfu Island (Ionian Islands, Greece), Quaternary International (2017), http://dx.doi.org/10.1016/j.quaint.2017.05.013

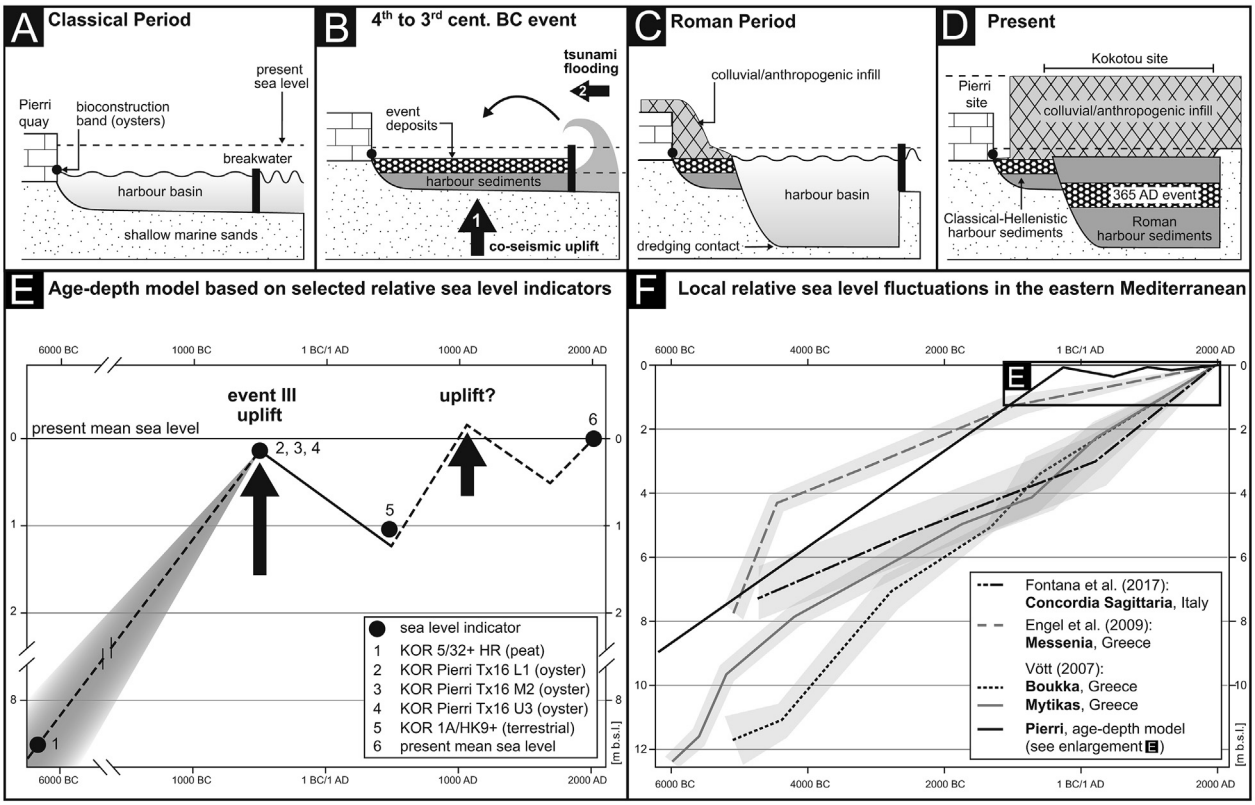

Fig. 12. Schematic palaeoenvironmental development of the Pierri harbour site. (A) The harbour of the Classical period developed from shallow marine conditions by protective harbour infrastructure, possibly breakwaters. Oyster colonization marked the approximate relative sea level at that time, resulting in a water depth of *c.* 1.2 m. (B) Between the 4th and 3rd century BC, the site experienced (i) co-seismic uplift causing decreasing water depths in the harbour, and, shortly afterwards, (ii) associated tsunami inundation. Due to co-seismic uplift and input of event deposits, the Classical-Hellenistic harbour was not navigable anymore. (C) During the Roman period, considerable parts of the buried Classical basin were deeply excavated, dredged and re-used, forming a more than 2 m deep harbour basin to the west of the Pierri site (Finkler et al., 2017). Comparing depths of the Classical and Roman harbour basins clearly reveals co-seismic uplift. (D) Today, harbour sediments of the Pierri site are covered by colluvial and anthropogenic material. Classical harbour infrastructure in form of a quay wall was found during archaeological excavations. (E) Age-depth model of selected relative sea level indicators from the Pierri site. Marine oysters dating to 335–183 cal BC were found on higher elevations than younger terrestrial material which causes a clear shift within the age-depth model. This break documents the co-seismic uplift of the Pierri site related to tsunami inundation of event III that occurred during Classical to Hellenistic times. It may be speculated that the time of dieback of oysters that took place between 335 and 183 cal BC represents the best-fit age estimate for this event. (F) Local relative sea level curves from different study sites (Vött, 2007; Engel et al., 2009; Fontana et al., 2017) in the eastern Mediterranean compared to relative sea level indicators encountered at the Pierri site.

zone of ancient Corcyra. We drilled three vibracores in the direct surrounding of the Pierri quay wall and ramp. Vibracores were investigated by means of a multi-proxy geoarchaeological approach comprising sedimentological, geochemical, micropalaeontological and geophysical methods. Our main conclusions can be summarized as follows:

(i) Based on vibracore stratigraphies, geoarchaeological studies and the archaeological context, we found that the quay wall segment and the ramp structure at Pierri belonged to a protected harbour basin. This harbour basin was developed from open littoral conditions of a shallow marine embayment most probably by the construction of breakwaters and/or other harbour facilities. Harbour deposits were dated by radiocarbon dating and archaeological age estimation of diagnostic ceramic fragments to the 4th to 3rd cent. BC which is in very good agreement with the quay wall structure which was dated to the Classical-Hellenistic period.

(ii) The harbour basin associated with the harbour infrastructure at the Pierri site was possibly in function even before the 4th cent. BC; older harbour sediments may have been removed by dredging, traces of which were detected right in front of the presumed ramp structure.

(iii) The geological archives in the study area revealed three distinct periods of time when the Pierri site, still part of a shallow marine embayment or used as a harbour, was hit by tsunami landfall, namely before 2483–2400 cal BC (event I), after 2483–2400 cal BC and before 370–214 cal BC (event II), and during Classical to Hellenistic times, most probably during the 4th to 3rd cent. BC (event III). Another tsunami event (event IV) potentially hit the site when it was already dry land. Ages of tsunami events I-II and candidate tsunami IV are consistent with supra-regional tsunamis known from the coasts of western Greece and southern Italy. Corresponding deposits at the Pierri site are thus triggered by teletsunamis.

(iv) Tsunami event III, dated to Classical to Hellenistic times, most probably to the 4th to 3rd cent. BC, must be regarded as associated to a local earthquake. Archaeoseismological features and sedimentary evidence of associated co-seismic uplift were found. By this event, the Pierri harbour site was uplifted and buried by event deposits so that it was not usable as a harbour any more. The site was then covered by anthropogenic debris and colluvial deposits, eroded from the hills of the Analipsis Peninsula.

(v) Finally, our results document that vertical crust uplift of the west coast of Corfu during event III exceeded crust uplift of

Please cite this article in press as: Finkler, C., et al., Geoarchaeological investigations of a prominent quay wall in ancient Corcyra – Implications for harbour development, palaeoenvironmental changes and tectonic geomorphology of Corfu Island (Ionian Islands, Greece), Quaternary International (2017), http://dx.doi.org/10.1016/j.quaint.2017.05.013

the east coast by c. 1.74 m. This means that Corfu Island was strongly tilted from west to east within the course of the local earthquake and tsunami event III.

Acknowledgements

The present study was undertaken within the framework of an interdisciplinary project directed by the Ephorate of Antiquities of Corfu, in collaboration with the Institute of Geography at the Johannes Gutenberg-Universität Mainz, Germany, associated with the Centre Camille Jullian, CNRS at the Aix-Marseille Université, France. We are kindly indebted to the personnel of the Ephorate of Antiquities of Corfu, for their various support during field work and their precious help. We would also like to thank the Pierri family, especially Mrs. Maria Pierri, as well as the authorities of the nearby Ag. Iason and Sosipatros church for their support and kind assistance. Finally, we would like to thank the Institute for Geology and Mineral Exploration (IGME, Athens) for the issue of work permits and the Deutsche Forschungsgemeinschaft (DFG) for funding the project (FI 1941/4-1 and VO 938/22-1).

References

Albini, P., 2004. A survey of the past earthquakes in the Eastern Adriatic (14th to early 19th century). Ann. Geophys. 47, 675–703.

Ambraseys, N., Synolakis, C., 2010. Tsunami catalogs for the eastern mediterranean, revisited. J. Earthq. Eng. 14, 309–330.

Argyraki, A., Ramsey, M.H., Potts, P.J., 1997. Evaluation of portable x-ray fluorescence instrumentation for in situ measurements of lead on contaminated land. Anal 122, 743–749.

Babbucci, D., Tamburelli, C., Viti, M., Mantovani, E., Albarello, D., D'Onza, F., Cenni, N., Mugnaioli, E., 2004. Relative motion of the Adriatic with respect to the confining plates: seismological and geodetic constraints. Geophys. J. Int. 159, 765–775.

Bahlburg, H., Weiss, R., 2007. Sedimentology of the December 26, 2004, Sumatra tsunami deposits in eastern India (Tamil Nadu) and Kenya. Int. J. Earth Sci. 96, 1195–1209.

Baika, K., 2003. ΝΕΩΣΟΙΚΟΙ. Installations navales en Méditerranée. Les neoria de Corcyre. Unpublished Ph.D. Thesis. Université de Paris I (Panthéon-Sorbonne), Paris.

Baika, K., 2013a. Corcyra (Corfu). In: Blackman, D., Rankov, B., Baika, K., Gerding, H., Pakkanen, J. (Eds.), Shipsheds of the Ancient Mediterranean. Cambridge University Press, Cambridge, pp. 319–334.

Baika, K., 2013b. The topography of shipshed complexes and naval dockyards. In: Blackman, D., Rankov, B., Baika, K., Gerding, H., Pakkanen, J. (Eds.), Shipsheds of the Ancient Mediterranean. Cambridge University Press, Cambridge, pp. 185–209.

Baika, K., 2015. Ancient harbour cities – new methodological perspectives and recent research in Greece. In: Ladstätter, S., Pirson, F., Schmidts, T. (Eds.), Harbors and Harbor Cities in the Eastern Mediterranean from Antiquity to the Byzantine Period, Volume I (= BYZAS 19). Ege Yayinlari, Istanbul, pp. 445–492.

Billi, A., Gambini, R., Nicolai, C., Storti, F., 2007. Neogene-Quaternary intraforeland transpression along a Mesozoic platform-basin margin: the Gargano fault system, Adria, Italy. Geosphere 3 (1), 1–15.

Blackman, D., 1982. Ancient harbours in the mediterranean. Part 2. Int. J. Naut. Archaeol. Underw. Explor. 11, 185–211.

Blackman, D., 2013. Classical and hellenistic sheds. In: Blackman, D., Rankov, B., Baika, K., Gerding, H., Pakkanen, J. (Eds.), Shipsheds of the Ancient Mediterranean. Cambridge University Press, Cambridge, pp. 16–29.

Bony, G., Marriner, N., Morhange, C., Kaniewski, D., Perinçek, D., 2012. A high-energy deposit in the Byzantine harbour of Yenikapı, Istanbul (Turkey). Quat. Int. 266, 117–130.

Blume, H.-P., Stahr, K., Leinweber, P., 2011. Bodenkundliches Praktikum. Spektrum, Heidelberg.

Brännvall, M.-L., Bindler, R., Emteryd, O., Renberg, I., 2001. Four thousand years of atmospheric lead pollution in northern Europe: a summary from Swedish lake sediments. J. Paleolimnol. 25, 421–435.

Brückner, H., Kelterbaum, D., Marunchak, O., Porotov, A., Vött, A., 2010. The Holocene sea level story since 7500 BP – lessons from the eastern mediterranean, the black and the azov seas. Quart. Int. 225 (2), 160–179.

Cavaleri, L., 2005. The wind and wave atlas of the Mediterranean Sea – the calibration phase. Adv. Geosci. 2, 255–257.

Cavicchia, L., von Storch, H., Gualdi, S., 2014. A long-term climatology of medicanes. Clim. Dyn. 43, 1183–1195.

Chagué-Goff, C., Goff, J., Wong, H.K.Y., Cisternas, M., 2015. Insights from geochemistry and diatoms to characterise a tsunami's deposit and maximum inundation limit. Mar. Geol. 359, 22–34.

Chagué-Goff, C., Szczuciński, W., Shinozaki, T., 2017. Applications of geochemistry in tsunami research: a review. Earth Sci. Rev. 165, 203–244.

Cimermann, F., Langer, M.R., 1991. Mediterranean Formaminifera. Slovenska Akademija Znanosti in Umetnosti, Ljubljana.

Davolio, S., Miglietta, M.M., Moscatello, A., Pacifico, F., Buzzi, A., Rotunno, R., 2009. Numerical forecast and analysis of a tropical-like cyclone in the Ionian Sea. Nat. Hazards Earth Syst. Sci. 9, 551–562.

D'Agostini, N., Avallone, A., Cheloni, D., D'Anastasio, E., Mantenuto, S., 2008. Active tectonics of the Adriatic region from GPS and earthquake slip vectors. J. Geophys. Res. Solid Earth 113, B12413.

Delile, H., Blichert-Toft, J., Goiran, J.-P., Keay, S., Albarède, F., 2014. Lead in ancient Rome's city waters. Proc. Natl. Acad. Sci. 111, 6594–6599.

De Martini, P.M., Burrato, P., Pantosti, D., Maramai, A., Graziani, L., Abramson, H., 2003. Identification of tsunami deposits and liquefaction features in the Gargano area (Italy): paleoseismological implication. Ann. Geophys. 46 (5), 883–902.

De Martini, P.M., Barbano, M.S., Pantosti, D., Smedile, A., Pirrotta, C., Del Carlo, P., Pinzi, S., 2012. Geological evidence for paleotsunamis along eastern Sicily (Italy): an overview. Nat. Hazards Earth Syst. Sci. 12, 2569–2580.

Di Bucci, D., Angeloni, P., 2013. Adria seismicity and seismotectonics: review and critical discussion. Mar. Pet. Geol. 42, 182–190.

DIN ISO 11277, 2002. Bodenbeschaffenheit - Bestimmung der Partikelgrößenverteilung in Mineralböden - Verfahren mittels Siebung und Sedimentation. ISO 11277:1998 and ISO 11277, Corrigendum 1. Beuth Verlag GmbH, Berlin.

Dominey-Howes, D., Cundy, A., Croudace, I., 2000. High energy marine flood deposits on Astypalaea Island, Greece: possible evidence for the AD 1956 southern Aegean tsunami. Mar. Geol. 163, 303–315.

Dontas, G., 1965. Τοπογραφικά θέματα της πολιορκίας της Κέρκυρας του έτους 373 π. χ. (Topographical issues of the siege of Corcyra in 373 BC). Archaiologiki Ephimeris 1965, 139–144.

Doutsos, T., Kokkalas, S., 2001. Stress and deformation patterns in the Aegean region. J. Struct. Geol. 23, 455–472.

Elmaleh, A., Galy, A., Allard, T., Dairon, R., Day, J.A., Michel, F., Marriner, N., Morhange, C., Couffignal, F., 2012. Anthropogenic accumulation of metals and metalloids in carbonate-rich sediments: insights from the ancient harbor setting of Tyre (Lebanon). Geochim. Cosmochim. Acta 82, 23–38.

Engel, M., Knipping, M., Brückner, H., Kiderlen, M., Kraft, J.C., 2009. Reconstructing middle to late Holocene palaeogeographies of the lower Messenian plain (southwestern Peloponnese, Greece): coastline migration, vegetation history, and sea level change. Palaeogeogr. Palaeoclimatol. Palaeoecol. 284, 257–270.

EPA - U.S. Environmental Protection Agency, 2007. Method 6200: Field Portable X-ray Fluorescence Spectrometry for the Determination of Elemental Concentrations in Soil and Sediment. www.epa.gov/hw-sw846/sw-846-test-method-6200-field-portable-x-ray-fluorescence-spectrometry-determination (last Access on 20 March 2017).

Evelpidou, N., Karkani, A., Pirazzoli, P.A., 2014. Fossil shorelines at Corfu and surrounding islands deduced from erosional notches. Holocene 24, 1565–1572.

Ferentinos, G., Gkioni, M., Geraga, M., Papatheodorou, G., 2012. Early seafaring activity in the southern ionian islands, mediterranean sea. J. Archaeol. Sci. 39, 2167–2176.

Finkler, C., Fischer, P., Baika, K., Rigakou, D., Metallinou, G., Hadler, H., Vött, A., 2017. Tracing the Alkinoos Harbour of ancient Kerkyra, Greece, and reconstructing its palaeotsunami history. Geoarchaeology 1–19. http://dx.doi.org/10.1002/gea.21609.

Fischer, P., Finkler, C., Röbke, B.R., Baika, K., Hadler, H., Willershäuser, T., Rigakou, D., Metallinou, G., Vött, A., 2016a. Impact of Holocene tsunamis detected in lagoonal environments on Corfu (Ionian Islands, Greece) – geomorphological, sedimentary and microfaunal evidence. Quat. Int. 401, 4–16.

Fischer, P., Wunderlich, T., Rabbel, W., Vött, A., Willershäuser, T., Baika, K., Rigakou, D., Metallinou, G., 2016b. Combined electrical resistivity tomography (ERT), direct-push electrical conductivity (DP-EC) logging and coring – a new methodological approach in geoarchaeological research. Archaeol. Prospect. 23 (3), 213–228.

Fontana, A., Vinci, G., Tasca, G., Mozzi, P., Vacchi, M., Bivi, G., Salvador, S., Rossato, S., Antonioli, F., Asioli, A., Bresolin, M., Di Mario, F., Hajdas, I., 2017. Lagoonal settlements and relative sea level during Bronze Age in Northern Adriatic: geoarchaeological evidence and paleogeographic constraints. Quat. Int. 2017, 1–20. http://dx.doi.org/10.1016/j.quaint.2016.12.038.

Fujiwara, O., Masudab, F., Sakaib, T., Irizukic, T., Fused, K., 2000. Tsunami deposits in Holocene bay mud in southern Kanto region,Pacific coast of central Japan. Sediment. Geol. 135, 219–230.

GEBCO (General Bathymetric Chart of the Oceans), 2014. The GEBCO_2014 Grid. www.gebco.net (last Access on 28 April 2015).

Gehrke, H.-J., Wirbelauer, E., 2004. Korkyra. In: Hansen, M.H., Nielsen, T.H. (Eds.), An Inventory of Archaic and Classical Poleis. Oxford University Press, Oxford and New York, pp. 361–363.

Gelfenbaum, G., Jaffe, B., 2003. Erosion and sedimentation from the 17 July, 1998 Papua New Guinea tsunami. Pure Appl. Geophys. 160, 1969–1999.

Geyh, M.A., 2005. Handbuch der physikalischen und chemischen Alterbestimmung. Wissenschaftliche Buchgesellschaft, Darmstadt.

Ghionis, G., Poulos, S.E., Verykiou, E., Karditsa, A., Alexandrakis, G., Andris, P., 2015. The impact of an extreme storm event on the barrier beach of the Lefkada Lagoon,NE ionian sea (Greece). Mediterr. Mar. Sci. 16 (3), 562–572.

Gianfreda, F., Mastronuszzi, G., Sansó, P., 2001. Impact of historical tsunamis on a sandy coastal barrier:an example from the northern Gargano coast, southern

Italy. Nat. Hazards Earth Syst. Sci. 1, 213–219.
Goff, J., Chagué-Goff, C., Nichol, S., 2001. Palaeotsunami deposits: a New Zealand perspective. Sediment. Geol. 143, 1–6.
Hadler, H., Vött, A., Brückner, H., Bareth, G., Ntageretzis, K., Warnecke, H., Willershäuser, T., 2011. The harbour of ancient Krane, Kutavos Bay (Cefalonia, Greece) – an excellent geo-archive for palaeo-tsunami research. In: Karius, V., Hadler, H., Deicke, M., Van Eynatter, H., Brückner, H., Vött, A. (Eds.), Dynamische Küsten – Grundlagen, Zusammenhänge und Auswirkungen im Spiegel angewandter Küstenforschung, pp. 111–122. Coastline Reports 17, Rostock.
Hadler, H., Willershäuser, T., Ntageretzis, K., Henning, P., Vött, A., 2012. Catalogue entries and non-entries of earthquake and tsunami events in the Ionian Sea and the Gulf of Corinth (eastern Mediterranean, Greece) and their interpretation with regard to palaeotsunami research. In: Vött, A., Venzke, J.-F. (Eds.), Beiträge der 29. Jahrestagung des Arbeitskreises „Geographie der Meere und Küsten", 28. bis 30. April 2011 in Bremen, Bremer Beiträge zur Geographie und Raumplanung, vol. 44, pp. 1–15.
Hadler, H., Vött, A., Koster, B., Mathes-Schmidt, M., Mattern, T., Ntageretzis, K., Reicherter, K., Willershäuser, T., 2013. Multiple late-Holocene tsunami landfall in the eastern Gulf of Corinth recorded in the palaeotsunami geo-archive at Lechaion, harbour of ancient Corinth (Peloponnese, Greece). Z. für Geomorphol. N.F. Suppl. Issue 57 (4), 139–180.
Hadler, H., Baika, K., Pakkanen, J., Evangelistis, D., Emde, K., Fischer, P., Ntageretzis, K., Röbke, B., Willershäuser, T., Vött, A., 2015. Palaeotsunami impact on the ancient harbour site Kyllini (western Peloponnese, Greece) based on a geomorphological multi-proxy approach. Z. für Geomoprhologie Suppl. Issue 59 (4), 7–41.
Harrington, G.A., Hendry, M.J., 2006. Using direct-push EC logging to delineate heterogeneity in a clay-rich aquitard. Ground Water Monit. Remediat. 26 (1), 92–100.
Hawkes, A.D., Bird, M., Cowie, S., Grundy-Warr, C., Horton, B.P., Hwai, A.T.S., Law, L., Macgregor, C., Nott, J., Ong, J.E., Rigg, J., Robinson, R., Tab-Mullins, M., Tiong Sa, T., Yasin, Z., Aik, L.W., 2007. Sediments deposited by the 2004 indian ocean tsunami along the Malaysia–Thailand peninsula. Mar. Geol. 242, 169–190.
Hollenstein, C., Müller, M., Geiger, A., Kahle, H.G., 2008. Crustal motion and deformation in Greece from a decade of GPS measurements, 1993 – 2003. Tectonophysics 449, 17–40.
Hong, S., Candelone, J.-P., Patterson, C.C., Boutron, C.F., 1994. Greenland ice evidence of hemispheric lead pollution two millennia ago by Greek and roman civilizations. Science 265, 1841–1843.
IGME - Institute of Geology and Mineral Exploration, 1970. In: Geological Map of Greece – Sheet North and South Corfu. Scale 1:50.000. Athens.
Judd, K., Chagué-Goff, C., Goff, J., Gadd, P., Zawadzki, A., Fierri, D., 2017. Multi-proxy evidence for small historical tsunamis leaving little or no sedimentary record. Mar. Geol. 385, 204–215.
Kanta-Kitsou, A., 2001. Ένας νεώσοικος, τμήμα των νεωρίων του Υλλαϊκού λιμανιού της Αρχαίας Κέρκυρας (A shipshed, section of the neorion of the Hyllaikos Harbour of ancient Corcyra). In: Tzalas, H., Tropis, V.I. (Eds.), Proceedings of the 6th International Symposium on Ship Construction in Antiquity, Lamia 1996. Hellenic Institute for the Preservation of Nautical Tradition, Athens, pp. 273–299.
Karathanasi, F., Soukissian, T., Sifnioti, D., 2015. Offshore wave potential of the mediterranean sea. Renew. Energy Power Qual. J. 13.
Köhn, M., 1929. Korngrößenbestimmung vermittels pipettanalyse. Tonindustrie-Zeitung 55, 729–731.
Kokkalas, S., Xypolias, P., Koukouvelas, I., Doutsos, T., 2006. Postcollisional contractional and extensional deformation in the Aegean region. In: Dilek, Y., Pavlides, S. (Eds.), Postcollisional Tectonics and Magmatism in the Mediterranean Region and Asia, Geological Society of America Special Paper, vol. 409, pp. 97–123.
Kiechle, F.K., 1979. Korkyra und der Handelsweg durch das Adriatische Meer im 5. Jh. v. Chr. Historia: Zeitschrift für Alte Geschichte, vol. 28, pp. 173–191.
Lario, J., Luque, L., Zazo, C., Goy, J.L., Spencer, C., Cabero, A., Bardají, T., Borja, F., Dabrio, C.J., Civis, J., Gondzález-Delgado, J.A., Borja, C., Alonso-Azcárate, J., 2010. Tsunami vs. Storm surge deposits: a review of the sedimentological and geomoprhological records of extreme wave events (EWE) during the Holocene in the Gulf of Cadiz, Spain. Z. für Geomorphol. N.F. Suppl. Issue 54 (3), 301–316.
Lehmann-Hartleben, K., 1923. Die antiken Hafenanlagen des Mittelmeeres. Beiträge zur Geschichte des Städtebaus im Altertum. Klio: Beiträge zur alten Geschichte. Beiheft XIV. Dietrich'sche Verlagsbuchhandlung, Leipzig.
Le Roux, G., Véron, Morhange, C., 2003. Geochemical evidences of early anthropogenic activity in harbour sediments from Sidon. Archaeol. Hist. Leban. 18, 115–118.
Le Roux, G., Véron, A., Morhange, C., 2005. Lead pollution in the ancient harbours of Marseille. Méditerranée 1, 31–35.
Lessler, M.A., 1988. Lead and lead poisoning from antiquity to modern times. Ohio J. Sci. 88 (3), 78–84.
Lionello, P., Abrantes, F., Congedi, L., Dulac, M.G., Gomis, D., Goodess, C., Hoff, H., Kutiel, H., Luterbacher, J., Planton, S., Reale, M., Schröder, K., Struglia, M.V., Toreti, A., Tsimplis, M., Ulbrich, U., Xoplaki, E., 2012. Introduction: mediterranean climate – background information. In: Lionello, P. (Ed.), The Climate of the Mediterranean Region. From the Past to the Future. Elsevier, London (pp. xxxv-xc).
Llasat, M.C., 2009. High magnitude storms and floods. In: Woodward, J.C. (Ed.), The Physical Geography of the Mediterranean. University Press, Oxford, pp. 513–540.
Loeblich, A.R., Tappan, H.N., 1988. Foraminiferal Genera and Their Classification. Springer, New York.
Mamo, B., Strotz, L., Dominey-Howes, D., 2009. Tsunami sediments and their foraminiferal assemblages. Earth Sci. Rev. 96, 263–278.
Marinos, G., Sakellariou-Mane, E., 1964. Über das Alter der letzten Senkungen des Ionischen Meeres. Entdecken prehistorischen Schicht der Steinzeit in NW Korfu. Bull. Geol. Soc. Greece 6, 14–24.
Marriner, N., Morhange, C., 2006. The 'Ancient Harbour Parasequence': anthropogenic forcing of the stratigraphic highstand record. Sediment. Geol. 186, 13–17.
Marriner, N., Morhange, C., 2007. Geoscience of ancient Mediterranean harbours. Earth Sci. Rev. 80, 137–194.
Mastronuzzi, P., Sansò, P., 2012. The role of strong earthquakes and tsunami in the Late Holocene evolution of the Fortore River coastal plain (Apulia, Italy): a synthesis. Geomorphology 138 (1), 89–99.
Mastronuzzi, G., Pignatelli, C., Sansò, P., Selleri, G., 2007. Boulder accumulations produced by the 20th of February, 1743 tsunami along the coast of southeastern Salento (Apulia region, Italy). Mar. Geol. 242, 191–205.
Mastronuzzi, G., Calcagnile, L., Pignatelli, C., Quarta, G., Stamatopoulos, L., Venisti, N., 2014. Late Holocene tsunamigenic uplift in kerkira island, Greece. Quat. Int. 332, 48–60.
Mathes-Schmidt, M., Schwarzbauer, J., Papanikolaou, I., Syberberg, F., Thiele, A., Wittkopp, F., Reicherter, K., 2013. Geochemical and micropaleontological investigations of tsunamigenic layers along the thracian coast (northern aegean sea, Greece). Z. für Geomorphol. Suppl. Issue 57 (4), 5–27.
May, S.M., Vött, A., Brückner, H., Grapmayer, R., Handl, M., Wennrich, V., 2012. The Lefkada barrier and beachrock system (NW Greece) — controls on coastal evolution and the significance of extreme wave events. Geomorphology 139–140, 330–347.
Mazarakis, N., Kotroni, V., Lagouvardos, K., Bertotti, L., 2012. High-resolution wave model validation over the Greek maritime areas. Nat. Hazards Earth Syst. Sci. 12, 3433–3440.
Miglietta, M.M., Mastrangelo, D., Conte, D., 2015. Influence of physics parameterization schemes on thesimulation of a tropical-like cyclone in the Mediterranean Sea. Atmos. Res. 153, 360–375.
Morgan, C., 2010. Ionian islands, excluding kythera. Archaeol. Rep. 56, 67–72.
Morhange, C., Marriner, N., Carayon, N., 2014. The geoarchaeology of ancient Mediterranean harbours. In: Carcaud, N., Arnaud-Fassetta, G. (Eds.), La géoarchéologie française au XXIe siècle. CNRS Edition, Paris, pp. 245–254.
Morton, R.A., Gelfenbaum, G., Jaffe, B.E., 2007. Physical criteria for distinguishing sandy tsunami and storm deposits using modern examples. Sediment. Geol. 200, 184–207.
Murray, J.W., 1991. Ecology and Paleoecology of Benthic Foraminifera. Longman Scientific & technical, Essex.
Murray, J.W., 2006. Ecology and Applications of Benthic Foraminifera. Cambridge University Press, Cambridge.
NCMA S.A. – National Cadastre and Mapping Agency S.A, 2014. Orthophotos for Greece 2007-2009 (WMS-service). http://gis.ktimanet.gr/wms/ktbasemap/default.aspx (last Access on 02 February 2016.
Partsch, J., 1887. Die Insel Korfu. Eine Geographische Monographie. Petermanns Mitteilungen, Ergänzungsheft 88. Justus Perthes, Gotha.
Pilarczyk, J.E., Dura, T., Horton, B.P., Engelhart, S.E., Kemp, A.C., Sawai, Y., 2014. Microfossils from coastal environments as indicators of paleo-earthquakes, tsunamis and storms. Palaeogeogr. Palaeoclimatol. Palaeoecol. 413, 144–157.
Pirazzoli, P.A., Stiros, S.C., Laborel, J., Laborel-Deguen, F., Arnold, M., Papageorgiou, S., Morhange, C., 1994. Late-Holocene shoreline changes related to palaeoseismic events in the Ionian Islands, Greece. Holocene 4, 397–405.
Poulos, S.E., Lykousis, V., Collins, M.B., Rohling, E.J., Pattiaratchi, C.B., 1999. Sedimentation processes in a tectonically active environment: the Kerkyra-Kefalonia submarine valley system (NE Ionian Sea). Mar. Geol. 160, 25–44.
Preka-Alexandri, K., 1986. Κέρκυρα, ραλαιόπολη (Corcyra, palaiopoli). Archaiologikon Delt. 41 B, 125–129.
Reimer, P.J., McCormac, F.G., 2002. Marine radiocarbon reservoir corrections for the mediterranean and aegean seas. Radiocarbon 44, 159–166.
Reimer, P.J., Bard, E., Bayliss, A., Becks, J.W., Blackwell, P.G., Bronk Ramsey, C., Buck, C.E., Cheng, H., Edwards, R.L., Friedrich, M., Grootes, P.M., Guilderson, T.P., Haflidason, H., Hajdas, I., Harré, C., Heaton, T.J., Hoffmann, D.L., Hogg, A.G., Hughen, K.A., Kaiser, K.F., Kromer, B., Manning, S.W., Niu, M., Reimer, R.W., Richards, D.A., Scott, E.M., Southon, J.R., Staff, R.A., Turney, C.S.M., Van der Pflicht, J., 2013. INTCAL13 and MARINE13 radiocarbon age calibration curves 0-50,000 years cal BP. Radiocarbon 55, 1869–1887.
Riginos, G., Karamanou, A., Kanta, K., Metallinou, G., Zernioti, D., 2000. Η Αρχαία Κέρκυρα - Πόλη και Ύπαιθρος- Μέσα από τα πορίσματα των πρόσφατων ερευνών (Ancient Corcyra – city and rural area – from the results of the recent investigations). In: Proceedings of the 6th International Panionian Conference, Volume 1, Thessaloniki, pp. 125–138.
Sachpazi, M., Hirn, A., Clément, C., Haslinger, F., Laigle, M., Kissling, E., Charvis, P., Hello, Y., Lépine, J.-C., Sapin, M., Ansorge, J., 2000. Western Hellenic subduction and Cephalonia Transform: local earthquakes and plate transport and strain. Tectonophysics 319, 301–319.
Sakuna, D., Szczuciński, W., Feldens, P., Schwarzer, K., Khokiattiwong, S., 2012. Sedimentary deposits left by the 2004 Indian Ocean tsunami on the inner continental shelf offshore of Khao Lak, Andaman Sea (Thailand). Earth Planets Space 64, 931–943.
Sapirstein, P., 2012. The monumental archaic roof of the temple of Hera at mon repos, Corfu. J. Am. Sch. Class. Stud. A. T. Athens 81 (1), 31–61.

Please cite this article in press as: Finkler, C., et al., Geoarchaeological investigations of a prominent quay wall in ancient Corcyra – Implications for harbour development, palaeoenvironmental changes and tectonic geomorphology of Corfu Island (Ionian Islands, Greece), Quaternary International (2017), http://dx.doi.org/10.1016/j.quaint.2017.05.013

Schulmeister, M.K., Butler, J.J., Healey, J.M., Zheng, L., Wysocki, D.A., McCall, G.W., 2003. Direct-push electrical conductivity logging for high-resolution hydrostratigraphic characterization. Ground Water Monit. Remediat. 23 (3), 52–62.

Scicchitano, G., Monaco, C., Tortorici, L., 2007. Large boulder deposits by tsunami waves along the Ionian coast of south-eastern Sicily (Italy). Mar. Geol. 238, 75–91.

Schmidt, B., 1890. Korkyräische Studien: Beiträge zur Topographie Korkyras und zur Erklärung des Thukydides. Xenophon und Diodoros, Teubner, Leipzig.

Shefsky, S., 1997. Comparing field portable x-ray fluorescence (XRF) to laboratory analysis of heavy metals. In: Soil. International Symposium of Field Screening Methods for Hazardous Wastes and Toxic Chemicals. Las Vegas, Nevada, USA. https://clu-in.org/download/char/dataquality/sshefsky02.pdf (last Access on 16 October 2016).

Sen Gupta, B.K.S., 1999. Modern Foraminifera. Kluwer Academic Publisher, Dordrecht.

Shi, S., Dawson, A., Smith, D., 1995. Coastal sedimentation associated with the december 12th, 1992 tsunami in flores, Indonesia. Pure Appl. Geophys. 144 (3/4), 525–536.

Smedile, A., De Martini, P.M., Pantosti, D., Bellucci, L., Del Carlo, P., Gasperini, L., Pirrotta, C., Polonia, A., Boschi, E., 2011. Possible tsunami signatures from an integrated study in the Augusta Bay offshore (Eastern Sicily—Italy). Mar. Geol. 281, 1–13.

Soloviev, S.L., Solovieva, O.N., Go, C.N., Kim, K.S., Shchetnikov, N.A., 2000. Tsunamis in the Mediterranean Sea 2000 B.C.-2000 A.D. Kluwer Academic Publishers, Dordrecht.

Spetsieri-Choremi, A., 1997. Ancient Kerkyra. Unpublished Report. Archaeological Receipts Fund, Ministry of Culture, Athens.

Stiros, S.C., Blackman, D.J., 2014. Seismic coastal uplift and subsidence in Rhodes Island, Aegean Arc: evidence from an uplifted ancient harbour. Tectonphysics 611, 114–120.

Stock, F., Knipping, M., Pint, A., Ladstätter, S., Delile, H., Heiss, A.G., Laermanns, H., Mitchell, P.D., Ployer, R., Steskal, M., Thanheiser, U., Urz, R., Wennrich, V., Brückner, H., 2016. Human impact on Holocene sediment dynamics in the Eastern Mediterranean – the example of the Roman harbour of Ephesus. Earth Surf. Process. Landforms 41 (7), 980–996.

Stucchi, M., Rovida, A., Gomez Capera, A.A., Alexandre, P., Camelbeeck, T., Demircioglu, M.B., Gasperini, P., Kouskouna, V., Musson, R.M.W., Radulian, M., Sesetyan, K., Vilanova, S., Baumont, D., Bungum, H., Fäh, D., Lenhardt, W., Makropoulos, K., Martinze Solares, J.M., Scotti, J., Živčić, M., Albini, P., Batllo, J., Papaioannou, C., Tatevossian, R., Locati, M., Meletti, C., Viganò, D., Giardini, D., 2013. The SHARE european earthquake catalogue (SHEEC) 1000–1899. J. Seismol. 17, 523–544.

Stuiver, M., Reimer, P.J., 1993. Extended 14C data base and revised Calib 3.0 14C age calibration program. Radiocarbon 35, 215–230.

Suric, M., Korbar, T., Juračić, M., 2014. Tectonic constraints on the late Pleistocene-Holocene relative sea-level change along the north-eastern Adriatic coast (Croatia). Geomorphology 220, 93–103.

Switzer, A.D., Jones, B.G., 2008. Large-scale washover sedimentation in a freshwater lagoon from the southeast Australian coast: sea-level change, tsunami or exceptionally large storm? Holocene 18, 787–803.

Thucydides after Dent, J.M., 1910. The Peloponnesian War. Translated by Richard Crawley. E.P. Dutton, New York.

van Hinsbergen, D.J.J., van der Meer, D.G., Zachariasse, W.J., Meulenkamp, J.E., 2006. Deformation of western Greece during Neogene clockwise rotation and collision with Apulia. Int. J. Earth Sci. 95, 463–490.

Véron, A., Goiran, J.P., Morhange, C., Marriner, N., Empereur, J.Y., 2006. Pollutant lead reveals the pre-Hellenistic occupation and ancient growth of Alexandria, Egypt. Geophys. Res. Lett. 33, L06409.

Vött, A., Brückner, H., 2006. Versunkene Häfen im Mittelmeerraum. Geogr. Rundsch. 58 (4), 12–21.

Vött, A., 2007. Relative sea level changes and regional tectonic evolution of seven coastal areas in NW Greece since the mid-Holocene. Quart. Sci. Rev. 26 (7–8), 894–919.

Vött, A., May, M., Brückner, H., Brockmüller, S., 2006. Sedimentary evidence of late Holocene tsunami events near Lefkada island (NW Greece). Z. für Geomorphol. N.F. Suppl. Vol. 146, 139–172.

Vött, A., Brückner, H., May, S.M., Sakellariou, D., Nelle, O., Lang, F., Kapsimalis, V., Jahns, S., Herd, R., Handl, M., Fountoulis, I., 2009. The Lake Voulkaria (Akarnania, NW Greece) palaeoenvironmental archive – a sediment trap for multiple tsunami impact since the mid- Holocene. Z. für Geomorphol. N.F. Suppl. Issue 53 (1), 1–37.

Vött, A., Bareth, G., Brückner, H., Curdt, C., Fountoulis, I., Grapmayer, R., Hadler, H., Hoffmeister, D., Klasen, N., Lang, F., Masberg, P., May, S.M., Ntageretzis, K., Sakellariou, D., Willershäuser, T., 2010. Beachrock-type calcarenitic tsunamites along the shores of the eastern Ionian Sea (western Greece) – case studies from Akarnania, the Ionian Islands and the western Peloponnese. Z. für Geomorphol. N.F. Suppl. Issue 54 (3), 1–50.

Vött, A., Bareth, G., Brückner, H., Lang, F., Sakellariou, D., Hadler, H., Ntageretzis, K., Willershäuser, T., 2011a. Olympia's harbour site pheia (elis, western peloponnese, Greece). Destroyed by tsunami impact. Die Erde 142, 259–288.

Vött, A., Lang, F., Brückner, H., Gaki-Papanastassiou, K., Maroukian, H., Papanastassiou, D., Giannikos, A., Hadler, H., Handl, M., Ntageretzis, K., Willershäuser, T., Zander, A., 2011b. Sedimentological and geoarchaeological evidence of multiple tsunamigenic imprint on the Bay of Palairos-Pogonia (Akarnania, NW Greece). Quat. Int. 242, 213–239.

Vött, A., Fischer, P., Röbke, B.R., Werner, V., Finkler, C., Hadler, H., Handl, M., Ntageretzis, K., Willershäuser, T., 2015. Holocene fan alluviation and terrace formation by repeated tsunami passage at Epitalio near Olympia (Alpheios River valley, Greece). Z. für Geomorphol. N.F. Suppl. Issue 59 (4), 81–123.

Walker, M., 2005. Quaternary Dating Methods. Wiley, Chichester.

Willershäuser, T., Vött, A., Brückner, H., Bareth, G., Nelle, O., Nadeau, M.-J., Hadler, H., Ntageretzis, K., 2013. Holocene tsunami landfalls along the shores of the inner Gulf of argostoli (Cefalonia island, Greece). Z. für Geomorphol. N.F. Suppl. Issue 57 (4), 105–138.

Zacharioudaki, A., Korres, G., Perivoliotis, L., 2015. Wave climate of the Hellenic Seas obtained from a wavehindcast for the period 1960–2001. Ocean. Dyn. 65, 795–816.

Please cite this article in press as: Finkler, C., et al., Geoarchaeological investigations of a prominent quay wall in ancient Corcyra – Implications for harbour development, palaeoenvironmental changes and tectonic geomorphology of Corfu Island (Ionian Islands, Greece), Quaternary International (2017), http://dx.doi.org/10.1016/j.quaint.2017.05.013